Appendix A

The spectral channel outputs obtained after "sky subtraction" are only proportional to the radiation temperatures and that too modulated by individual channel gains. These channel gains are calibrated using the channel outputs obtained by observing an ambient temperature absorber once every few minutes. Thus a simple observing sequence is made of three sets of measurements: ON, OFF and AMB. The first two correspond to measurements at two different sky-paitions (beam or position switching) or frequencies (frequency switching) and the last to measurements with the beam completely blocked by the absorber.

Let V_{on}, V_{off} and V_{amb} be the respective measured voltage outputs from a given spectral channel. Let the signal and image band system gains in that channel be G_s and G_i respectively. Then for a spectral line observation with a double side-band (DSB) system,

$$V_{on} = G_s T_{sys,s} + G_i T_{sys,i} + G_s T_{source}$$

$$V_{off} = G_s T_{sys,s} + G_i T_{sys,i}$$

$$V_{amb} = G_s T_{sys,s} + G_i T_{sys,i} + (G_s + G_i) T_{amb}$$

Here $T_{sys,s}$ and $T_{sys,i}$ are the system temperatures, respectively, in the signal and image bands as measured outside the atmosphere. Solving for the source temperature one gets,

$$T_{source} = T_{amb}\left(1 + \frac{G_i}{G_s}\right)\frac{(V_{on} - V_{off})}{(V_{amb} - V_{off})}$$

T_{source} thus obtained is normally referred to as T_a^*, the antenna temperature of the source corrected for all telescope losses occuring at ambient temperatures (for example, an attenuating element in the beam path, or truncation of the beam due to or spillover onto ambient temperature objects). It is not corrected for that part of the telescope response on the sky outside the main beam due to spillover past the secondary, the error pattern etc.. This correction is done by dividing T_a^* by η_{fss}, the forward spillover and scattering efficiency, which may depend on the elevation of observation. This can be found by observing a calibration source filling the main beam with a well determined radiation temperature at various elevations. Then the ratio of the observed T_a^* to the expected radiation temperature gives the η_{fss} as a function of elevation. In this way, we find the zenith η_{fs} to be 0.57 and 0.61 at ^{12}CO and ^{13}CO frequencies, respectively, during our observations.

We conclude this appendix with a comment about the relative time budgeting among the various steps **viz.** ON, **OFF** and AMB measurements of the observing sequence. Let V_{on}, V_{off} and V_{amb} be the average values of the output of a given channel and N_{on}, N_{off} and N_{amb} the corresponding noise on them. Then these can be related to the noise on the measured T_{source}, N_s to the first order by

$$N_s = \frac{1}{(V_{on} - V_{off})}\left[N_{on} + N_{off} + (N_{amb} + N_{off})\frac{(V_{on} - V_{off})}{(V_{amb} - V_{off})}\right]$$

As will be seen, the contribution from the noise on the ambient measurement is weighted down by a factor equal to the ratio of the differences of the means viz. $V_{on} - V_{off}$ and $V_{amb} - V_{off}$. **Typically** this ratio is ≤ 10. Thus the equal portioning of the noise contribution to maximally use the time requires that the amounts of time spent on ON, **OFF** and AMB measurements be in the ratio of **100:100:1.** With a safety margin, we use a ratio of **300:300:20.** Even though the noise in the AMB measurements will be larger due to the relatively small fraction of time spent, it does not affect the noise on the calibrated spectra because of the following two reasons:

1. a small signal step is being calibrated by a large calibration step
2. the use of larger calibration step does not affect the noise on the measurements much which is largely decided by the receiver emission whose mean value is much larger than even the calibration step.

Appendix B

The details of the observed positions and the parameters derived from the observed spectra such as centre velocity, line strengths (T_a^*) and line widths are given in this Appendix. The coordinates for the northern clouds were taken from the catalogue of Taylor et al. (1987), and for the southern clouds from the catalogue of Feitzinger and Stuwe (1984). They are named GLD$\star\star\star$ and SDC$\star\star\star$, respectively, where $\star\star\star$ is a 3-digit serial number in the respective catalogues.

Locations of the clouds with associated reflection nebulae were obtained from the Palomar Observatory Sky Survey prints using the coordinates of the exciting stars listed by van den Bergh (1966). Sources named VDB are detected close to the stellar positions, while others were detected at positions offset with respect to the stars. In all cases the numbers indicate the serial number in the catalogue of van den Bergh.

Separate set of Tables are given for the northern and southern clouds observed. In each category, the lines-of-sight with single, double and triple components are tabulated separately. The sources are ordered in galactic longitude and latitude. In the case of lines-of-sight with only one component details of the ^{13}CO spectra, if available, are given in adjacent columns. If only the ^{13}CO spectra are available, corresponding ^{12}CO entries are left vacant. In the case of spectra with multiple components, details of the ^{13}CO spectra are given in the adjacent rows following their ^{12}CO counterparts.

NORTHERN CLOUDS

Source	lII	bII	V_{12}	$T^{\star}_{a,12}$	ΔV_{12}	rms	V_{13}	$T^{\star}_{a,13}$	ΔV_{13}	rms
GLD001	352.20	17.04	4.4	5.8	1.6	0.2				
GLD003	353.00	18.07	3.3	7.3	1.8	0.2				
GLD004	353.30	15.30	4.0	10.2	1.7	0.2				
GLD005	353.40	18.27	2.1	4.3	2.0	0.3	3.0	0.9	1.1	0.2
GLD006	353.90	16.90	2.5	11.7	1.4	0.2	2.5	2.8	1.3	0.1
GLD008	354.40	17.41	1.4	9.8	1.5	0.2	1.4	2.3	1.4	0.2
GLD015	357.80	15.45	2.0	10.1	1.7	0.3	2.0	6.0	1.2	0.2
GLD024	0.25	11.72	2.5	6.1	1.2	0.2	2.5	2.7	0.9	0.1
GLD027	0.53	10.34	4.4	9.7	1.6	0.2	4.5	5.4	1.3	0.2
GLD034	1.63	6.88	4.4	1.2	1.8	0.3				
GLD040	2.49	7.07	2.7	7.5	1.2	0.1	2.8	4.1	0.8	0.2
GLD088	11.11	3.37	6.4	5.0	1.9	0.2				
GLD092	11.63	−9.95	7.8	5.2	1.4	0.2				
GLD104	15.54	2.05	28.6	3.3	3.8	0.3				
GLD110	19.33	4.02	11.7	1.6	1.6	0.3				
GLD113	21.17	4.94					3.3	2.1	1.1	0.4
GLD123	23.13	4.87	6.1	3.0	4.1	0.2	6.3	1.7	2.2	0.1
GLD132	24.35	6.05					8.0	2.1	1.4	0.1
GLD134	24.45	−3.42	8.0	1.8	3.4	0.2				
GLD141	26.47	8.01	6.2	4.2	2.4	0.2				
GLD147	27.71	5.69	6.9	2.5	5.2	0.2				
GLD155	29.39	−4.83	10.5	1.1	1.9	0.2				
GLD157	29.68	−0.54	8.8	2.3	8.1	0.2				
GLD163	32.38	−15.30	3.2	4.2	1.1	0.2				
GLD169	35.31	6.28	8.5	1.5	1.6	0.2				
GLD173	35.70	−3.09	33.7	1.4	1.9	0.2				
GLD177	37.66	−2.08	6.5	3.5	1.4	0.2				
GLD185	43.01	8.37					4.0	1.8	1.3	0.1

Source	lII	bII	V_{12}	$T^{\star}_{a,12}$	ΔV_{12}	rms	V_{13}	$T^{\star}_{a,13}$	ΔV_{13}	rms
GLD189	44.28	−2.40	27.9	2.3	2.7	0.2				
GLD193	45.10	3.86	21.1	0.9	2.3	0.1				
GLD202	48.23	−5.73	9.1	3.9	1.3	0.2				
GLD207	49.49	−2.75	46.6	1.6	3.9	0.2				
GLD219	53.85	3.00	8.1	2.6	2.8	0.1				
GLD221	54.61	2.77	7.8	1.6	3.5	0.2	7.4	2.4	1.2	0.1
GLD222	54.64	2.79	8.0	1.7	3.5	0.2				
GLD227	55.51	3.83	8.8	5.5	1.6	0.1	8.7	2.4	1.3	0.2
GLD231	56.91	4.82	11.0	2.9	1.6	0.2	11.2	2.3	0.7	0.3
GLD232	57.11	4.45	10.6	3.9	1.2	0.1				
GLD233	57.12	3.65	11.2	5.8	2.7	0.1				
GLD235	57.28	4.03	10.9	4.7	1.6	0.2				
GLD237	57.39	2.43	11.4	3.3	1.7	0.2	11.5	2.0	1.2	0.1
GLD242	58.06	3.07	9.9	3.5	2.3	0.2				
GLD246	59.07	2.73	10.2	2.4	2.8	0.2				
GLD252	60.66	2.53	11.2	3.5	1.2	0.1				
GLD253	60.67	−0.30	30.7	3.0	2.6	0.1	30.4	1.4	1.8	0.1
GLD261	62.83	1.85	1.4	4.5	2.6	0.2				
GLD262	62.95	1.72	1.7	4.3	2.4	0.3				
GLD268	68.62	−3.43	9.2	2.7	4.2	0.2	9.7	1.1	2.1	0.1
GLD270	69.94	−2.66	3.4	3.2	2.1	0.3				
GLD272	70.57	−3.82	3.3	2.8	1.6	0.2	3.3	1.1	1.2	0.2
GLD273	70.67	−0.31	10.1	3.2	5.0	0.2	10.1	0.8	3.1	0.2
GLD276	71.13	−2.99	7.0	1.8	1.4	0.1				
GLD277	71.84	1.65	0.7	5.4	1.7	0.2				
GLD285	74.96	−0.02	2.3	1.2	9.0	0.2				
GLD289	76.52	1.03	16.2	2.4	1.9	0.2				
GLD293	78.20	1.27	0.6	4.5	3.1	0.2				
GLD300	83.75	−0.80					2.7	0.9	4.2	0.3

Source	lII	bII	V_{12}	$T^{\star}_{a,12}$	ΔV_{12}	rms	V_{13}	$T^{\star}_{a,13}$	ΔV_{13}	rms
GLD303	84.73	0.44	−2.3	8.4	3.7	0.2	−2.1	2.4	3.1	0.2
GLD304	84.76	−4.06	5.7	3.5	3.7	0.2	5.5	1.8	2.3	0.2
GLD305	84.83	−3.70	5.0	1.7	3.9	0.2	5.5	1.7	2.0	0.1
GLD308	85.19	−3.04	10.9	2.2	2.8	0.6				
GLD311	85.59	−2.62	10.0	2.9	3.2	0.2				
GLD312	85.60	−4.25	6.6	2.0	3.4	0.5				
GLD315	86.62	−1.93	12.3	2.0	5.0	0.2				
GLD316	86.86	−4.10	5.0	2.7	2.1	0.2	4.7	1.8	1.8	0.2
GLD317	86.88	−4.90	8.0	2.9	1.5	0.3				
GLD318	86.92	−2.02	12.5	2.4	3.5	0.3				
GLD319	86.92	−5.12	7.6	2.3	2.0	0.2				
GLD320	87.04	−2.54	13.0	3.5	2.5	0.3				
GLD322	87.36	−4.23	4.9	2.8	2.7	0.1				
GLD323	87.56	−4.38	5.0	2.4	1.4	0.2				
GLD325	89.66	−6.63	12.4	3.8	2.2	0.3	12.5	2.5	1.6	0.1
GLD326	89.70	2.21	−1.0	5.0	3.7	0.2				
GLD327	89.75	−6.93	12.3	5.0	2.3	0.2	12.6	2.2	1.7	0.1
GLD330	90.19	−2.16	4.9	5.2	3.0	0.2	5.0	4.1	1.6	0.2
GLD337	92.08	−1.16	5.2	4.0	1.9	0.2				
GLD340	92.56	−0.87	5.2	3.9	3.1	0.1	5.0	1.6	2.0	0.2
GLD347	93.62	−4.45	3.2	5.9	3.2	0.2	3.3	3.0	2.0	0.1
GLD352	94.31	−5.19					5.9	2.7	1.7	0.2
GLD353	94.46	−5.38	8.1	4.8	2.8	0.2	8.2	0.7	3.0	0.1
GLD362	97.09	10.11	−2.9	3.7	1.9	0.3				
GLD364	98.30	3.33	7.4	5.5	2.4	0.3				
GLD368	98.77	2.59	6.6	3.0	1.3	0.5	6.7	2.1	1.0	0.2
GLD371	99.13	2.87	5.0	2.7	1.9	0.2				
GLD373	99.61	4.14	−0.3	4.6	1.9	0.4				
GLD374	99.65	3.85	−1.1	3.3	1.6	0.3				

Source	lII	bII	V_{12}	$T^{\star}_{a,12}$	ΔV_{12}	rms	V_{13}	$T^{\star}_{a,13}$	ΔV_{13}	rms
GLD375	99.68	2.00	−2.8	3.0	2.3	0.2				
GLD377	100.40	8.82	0.4	7.4	2.2	0.4				
GLD378	100.80	5.17	−1.3	4.1	2.4	0.5				
GLD380	102.20	3.27	−2.0	5.0	3.4	0.3				
GLD381	102.20	8.31	1.9	4.4	4.1	0.2				
GLD384	102.40	2.70	−1.8	4.6	3.5	0.2	−1.7	1.6	2.3	0.3
GLD385	102.40	−0.54	−7.6	4.2	2.6	0.2	−7.4	1.4	2.2	0.1
GLD386	102.50	8.56	2.4	4.2	3.4	0.2				
GLD387	102.60	−0.36	−6.8	4.6	2.5	0.2	−6.7	2.1	1.7	0.1
GLD388	102.70	15.35	1.8	4.9	3.3	0.3				
GLD389	103.10	−15.17	3.1	3.6	1.8	0.1	3.5	1.3	1.4	0.2
GLD390	103.10	−17.13	−8.5	3.2	1.4	0.2	−8.6	0.9	1.1	0.1
GLD397	106.40	0.43	−3.3	3.1	1.8	0.1	−3.3	1.5	1.3	0.1
GLD402	107.30	−0.30	−3.5	3.2	2.6	0.3	−3.5	2.1	1.1	0.1
GLD403	107.30	4.46	−6.0	3.1	4.2	0.3	−6.4	1.1	2.8	0.4
GLD404	107.40	4.72	−4.5	4.7	2.4	0.5	−4.6	0.7	2.4	0.3
GLD407	109.40	6.71	−8.3	10.8	2.1	0.3	−8.4	5.1	1.6	0.3
GLD408	109.70	2.54	−9.1	6.8	2.8	0.3	−8.8	3.8	1.9	0.1
GLD410	110.30	11.41	−5.4	4.8	1.8	0.3	−5.1	2.8	1.2	0.1
GLD411	110.40	−12.63	−8.0	7.3	1.2	0.2	−7.9	4.1	1.0	0.2
GLD412	110.50	−12.60	−8.0	4.6	1.2	0.1	−7.9	1.3	2.6	0.3
GLD413	110.60	2.28	−10.5	8.0	4.4	0.2	−10.4	4.6	2.8	0.2
GLD414	110.60	11.96	−4.8	2.6	1.8	0.4				
GLD415	110.60	−12.57					−8.0	1.7	0.8	0.1
GLD416	110.60	9.72	−4.4	5.6	1.9	0.5				
GLD417	111.30	9.42	−7.8	6.0	1.5	0.4				
GLD418	111.40	2.01	−10.1	8.8	2.9	0.4	−10.2	3.8	1.9	0.1
GLD419	111.40	1.03	−11.3	5.1	2.0	0.3	−11.4	2.2	1.2	0.1
GLD424	112.00	0.46					−11.7	1.0	1.0	0.1

Source	lII	bII	V_{12}	$T^{\star}_{a,12}$	ΔV_{12}	rms	V_{13}	$T^{\star}_{a,13}$	ΔV_{13}	rms
GLD437	115.70	−3.16	−1.3	3.6	1.8	0.4	−1.4	1.2	1.4	0.2
GLD440	115.80	−3.54	−0.8	3.4	1.7	0.3	−0.9	2.8	1.6	0.1
GLD443	116.10	−2.40					−1.3	2.2	1.8	0.2
GLD445	116.20	−2.54	−0.9	3.6	2.5	0.5	−0.6	2.8	1.5	0.2
GLD447	117.10	12.40					3.7	3.1	1.2	0.3
GLD448	117.10	12.37	3.7	5.2	1.7	0.4	3.8	3.6	1.3	0.2
GLD450	117.80	9.58	−3.1	4.3	2.5	0.3	−2.8	2.3	1.5	0.2
GLD454	118.30	8.69	−2.7	4.6	2.5	0.5	−2.6	1.9	1.7	0.1
GLD456	118.60	3.75					−6.5	2.7	1.9	0.3
GLD457	119.20	7.82	−5.1	2.2	5.0	0.3	−5.1	0.7	1.8	0.3
GLD460	120.90	−3.83	−18.2	4.3	3.0	0.2	−17.8	3.3	1.7	0.2
GLD461	121.00	−9.97					−11.6	1.0	1.4	0.2
GLD463	121.40	0.68	−17.4	5.7	2.9	0.4	−17.2	2.5	2.1	0.3
GLD465	121.90	0.55	−18.6	2.7	2.2	0.4				
GLD466	121.90	−10.44	−9.5	3.9	2.4	0.2	−9.8	1.6	2.2	0.1
GLD470	122.20	−10.39	−10.7	5.3	1.3	0.2	−10.6	2.8	0.9	0.2
GLD471	122.20	−0.15	−18.1	6.0	2.4	0.4	−17.9	1.7	1.7	0.1
GLD473	122.80	9.64	2.9	3.4	2.1	0.4				
GLD475	123.90	−0.80					3.6	0.8	3.7	0.1
GLD478	124.90	−0.50					3.7	2.6	2.2	0.2
GLD485	127.00	−1.07	−12.6	4.1	3.9	0.3	−12.0	2.0	2.7	0.1
GLD486	127.30	13.51	2.8	2.6	3.9	0.5	2.9	1.5	2.6	0.2
GLD487	127.60	13.97	3.5	2.8	2.8	0.4	3.4	3.6	1.7	0.2
GLD488	127.90	2.66	−11.6	6.3	2.7	0.2	−11.4	3.1	1.8	0.1
GLD491	128.90	−0.20					−14.7	2.3	1.5	0.1
GLD492	129.90	11.61	−14.7	4.3	2.6	0.5	−14.3	1.8	2.2	0.2
GLD493	130.10	11.48	−15.5	5.5	2.2	0.5	−15.1	3.7	1.5	0.3
GLD494	132.30	13.25					−2.4	1.1	2.5	0.2
GLD498	134.00	0.79	−48.3	8.2	4.4	0.3	−48.0	4.5	3.6	0.2

Source	lII	bII	V_{12}	$T^{\star}_{a,12}$	ΔV_{12}	rms	V_{13}	$T^{\star}_{a,13}$	ΔV_{13}	rms
GLD499	136.40	0.71	–14.2	4.2	2.2	0.4				
GLD501	138.00	0.85	–38.3	3.8	2.1	0.3	–38.4	1.2	2.2	0.3
GLD502	138.00	1.77	–42.8	2.4	3.0	0.3	–42.8	0.7	2.9	0.2
GLD503	139.90	1.43	–11.3	2.2	1.1	0.4	–11.2	0.8	1.2	0.1
GLD506	140.80	2.28	–13.0	3.6	2.7	0.2				
GLD507	140.80	0.87	–38.8	2.2	3.2	0.2	2.8	0.8	3.0	0.2
GLD508	141.30	1.38	–10.3	3.6	2.1	0.3				
GLD510	141.80	2.58	–11.4	5.6	3.1	0.2	–11.3	2.2	1.9	0.3
GLD511	142.20	0.70					–15.4	2.3	2.8	0.1
GLD512	142.60	1.73	–12.9	4.4	4.0	0.3	–12.7	1.4	1.9	0.1
GLD513	142.90	1.31	–12.9	1.4	3.3	0.2				
GLD515	145.40	9.68	–13.0	3.2	1.4	0.2				
GLD522	149.50	3.42	3.2	4.0	2.1	0.3	3.2	2.9	1.4	0.3
GLD531	151.60	4.99	–6.5	3.5	1.9	0.3				
GLD541	154.10	5.24	3.7	3.7	2.4	0.3				
GLD544	155.00	4.64	3.3	5.5	2.4	0.2	3.2	2.7	1.6	0.4
GLD551	156.00	4.92	4.1	4.7	2.0	0.3				
GLD552	156.10	6.05	5.6	2.4	1.3	0.2				
GLD559	158.30	–8.29	–7.3	4.2	3.4	0.2				
GLD561	159.70	–11.93					1.2	0.8	2.0	0.1
GLD564	160.60	–1.24	–17.4	2.6	1.6	0.2				
GLD568	165.50	–9.08					–0.5	3.4	2.5	0.1
GLD573	168.30	–15.70	7.0	6.4	3.0	0.2				
GLD583	171.90	–5.24	7.1	3.7	1.4	0.1	6.9	2.5	0.7	0.1
GLD584	172.20	–16.95	6.7	5.0	2.4	0.2				
GLD587	172.70	–4.85	7.7	4.0	1.0	0.1				
GLD588	172.70	–14.56					6.0	2.0	1.6	0.2
GLD600	175.50	–12.21	5.7	4.8	2.9	0.1	5.7	1.4	2.1	0.1
GLD605	177.20	–15.15	4.1	1.0	3.6	0.2				

Source	lII	bII	V_{12}	$T^{\star}_{a,12}$	ΔV_{12}	rms	V_{13}	$T^{\star}_{a,13}$	ΔV_{13}	rms
GLD606	177.90	−9.77	7.0	4.5	1.4	0.2				
GLD607	178.50	−6.77	7.3	6.0	1.7	0.1				
GLD612	189.30	3.89	−2.4	2.2	3.1	0.2	−2.3	0.8	1.0	0.1
GLD613	191.20	−16.65					1.2	1.1	1.6	0.1
GLD614	191.50	−0.70	−0.5	3.7	2.3	0.1	−0.2	1.5	1.8	0.2
GLD615	192.00	−0.84	−1.4	3.3	3.4	0.1				
GLD616	192.30	−11.32	9.9	8.4	1.9	0.1				
GLD618	195.10	−16.43					−0.2	5.0	1.9	0.2
GLD622	197.00	−10.36	12.0	10.0	1.7	0.1	11.9	4.7	1.4	0.2
GLD625	201.40	−9.25	−40.0	0.6	0.8	0.1				
GLD630	206.50	1.30	15.9	3.0	1.6	0.2	16.0	1.6	1.2	0.2
GLD634	207.70	−1.86					13.8	1.4	2.9	0.1
GLD636	208.20	−19.54					9.9	0.8	2.9	0.1
GLD646	212.90	−12.30	12.3	5.7	3.0	0.3	12.3	2.0	1.7	0.1
GLD647	214.90	−12.80	10.9	3.6	4.1	0.1	11.6	1.8	2.2	0.1
GLD649	219.00	−8.75	11.2	3.6	2.2	0.1	11.4	1.8	1.3	0.2
GLD650	219.40	−9.54					12.2	1.7	1.1	0.4
GLD651	219.70	−10.78	11.7	1.8	2.6	0.1				
GLD653	224.30	−0.77	14.3	4.8	4.2	0.2	14.6	2.9	2.6	0.2
GLD654	224.40	−2.36	9.7	4.2	2.9	0.1				
GLD656	227.80	5.36	−30.1	0.8	3.3	0.2				
GLD658	236.40	−4.87	20.6	2.9	1.8	0.2				
GLD661	238.90	−1.65	18.6	3.7	2.9	0.3				
GLD662	240.10	−1.82	17.8	4.4	2.0	0.3				

NORTHERN CLOUDS WITH MULTIPLE COMPONENTS

Source	lII	bII		V_{12}	$T_a^\star$	ΔV	V_{12}	$T_a^\star$	ΔV	rms
				1st component			2nd component			
GLD002	352.90	16.69		2.3	16.6	1.5	4.3	9.8	2.0	0.2
GLD007	354.30	15.17		3.7	12.7	1.6	5.5	2.0	1.3	0.3
GLD042	2.71	3.16		2.8	7.4	1.7	4.9	1.8	2.7	0.3
GLD042	2.71	3.16	^{13}CO	2.7	2.0	1.1	4.6	0.5	1.6	0.1
GLD076	7.52	4.25		10.5	2.0	1.6	15.9	0.8	2.1	0.3
GLD076	7.52	4.25	^{13}CO	10.4	1.0	1.1				0.1
GLD096	13.60	5.20		9.2	2.0	2.4	12.3	1.4	2.8	0.2
GLD107	18.10	2.74		27.0	3.3	6.3	5.0	2.7	1.9	0.2
GLD119	22.35	3.20		4.2	2.1	2.5	7.2	2.8	4.2	0.2
GLD124	23.16	3.28		8.4	3.3	2.3	5.3	1.8	5.9	0.2
GLD124	23.16	3.28	^{13}CO	8.0	1.1	1.8				0.1
GLD136	25.24	7.83		6.6	3.6	2.7	11.2	1.3	2.1	0.1
GLD142	26.48	3.28		3.4	3.2	3.0	8.9	3.3	6.2	0.2
GLD201	47.80	5.08		13.2	1.7	3.5	17.0	1.1	1.4	0.2
GLD213	53.01	3.07		10.2	4.2	3.0	6.7	1.2	1.9	0.1
GLD223	54.67	3.14	^{13}CO	9.4	0.7	2.5	7.6	1.5	1.2	0.1
GLD224	54.69	3.63		7.8	1.2	1.9	6.1	0.9	6.4	0.2
GLD224	54.69	3.63	^{13}CO	7.4	1.0	2.3				0.3
GLD251	60.65	2.32		3.9	1.8	1.3	10.8	3.3	3.2	0.1
GLD269	69.11	−3.35		8.6	0.9	2.2	5.4	2.8	3.0	0.1
GLD269	69.11	−3.35	^{13}CO	5.0	0.7	1.7				0.2
GLD271	70.36	−1.68		11.6	3.8	5.1	9.0	3.4	2.3	0.1
GLD275	70.81	−2.17		7.9	1.7	2.2	2.8	0.8	3.1	0.1
GLD280	72.41	1.35		−3.8	2.6	2.1	6.0	2.2	2.0	0.2
GLD281	72.54	0.70		5.3	2.6	2.1	−11.0	1.9	1.5	0.2
GLD284	74.20	−5.11		10.8	1.6	4.3	16.6	0.7	1.1	0.2
GLD284	74.20	−5.11	^{13}CO	10.6	0.9	1.8				0.2

Source	lII	bII		V_{12}	$T_a^\star$	ΔV	V_{12}	$T_a^\star$	ΔV	rms
				1st component			2nd component			
GLD296	80.11	2.75		5.3	8.9	3.7				0.4
GLD296	80.11	2.75	^{13}CO	4.8	6.8	1.7	6.6	2.4	2.1	0.2
GLD298	82.95	1.53		3.5	2.6	6.3	13.1	4.1	2.0	0.2
GLD299	83.10	−1.76		3.6	2.9	3.0	−3.9	1.4	2.1	0.2
GLD301	84.47	−3.66		7.7	2.9	4.3	3.5	0.9	1.4	0.2
GLD301	84.47	−3.66	^{13}CO	7.8	0.9	2.9				0.1
GLD302	84.65	−1.08		3.3	5.1	6.6	7.0	1.9	1.5	0.2
GLD302	84.65	−1.08	^{13}CO	3.7	1.0	5.3	6.7	2.4	1.4	0.1
GLD309	85.41	−2.06		2.4	2.5	2.2	13.1	2.1	5.0	0.2
GLD321	87.08	−4.19		2.2	2.9	1.9	4.8	1.7	2.7	0.2
GLD321	87.08	−4.19	^{13}CO	4.4	0.7	3.4				0.1
GLD324	89.36	−0.69		2.2	3.8	4.6	5.9	−0.3	−1.0	0.2
GLD333	90.52	−1.49		2.8	2.7	1.9	5.0	1.6	3.0	0.2
GLD333	90.52	−1.49	^{13}CO	3.1	1.8	1.4				0.1
GLD335	91.65	4.88		−2.7	4.4	3.1	−5.4	3.9	2.2	0.2
GLD341	92.65	−0.13		3.5	3.6	2.9	9.0	1.5	3.3	0.2
GLD341	92.65	−0.13	^{13}CO	3.5	1.7	2.1				0.1
GLD342	93.03	3.37		−3.0	3.5	4.7	9.7	3.1	2.8	0.2
GLD383	102.40	3.02		−1.7	4.7	3.7	2.7	1.3	1.4	0.2
GLD391	103.20	2.76		−2.0	3.8	2.3	2.4	1.2	1.6	0.2
GLD396	105.60	1.15		−2.5	3.7	2.3	−0.1	2.7	0.6	0.2
GLD396	105.60	1.15	^{13}CO	−2.7	2.0	1.5				0.1
GLD399	106.90	5.32		−7.4	9.9	3.7	−9.4	6.1	2.0	0.2
GLD399	106.90	5.32	^{13}CO	−7.9	6.0	3.2				0.3
GLD401	107.20	5.22		−11.2	3.7	1.9	−8.7	1.6	5.5	0.2
GLD405	107.50	4.51		−1.9	5.8	4.2	0.8	2.3	1.7	0.2
GLD405	107.50	4.51	^{13}CO	−1.4	4.9	3.0				0.4

Source	lII	bII		V_{12}	T_a^*	ΔV	V_{12}	T_a^*	ΔV	rms
				1st component			2nd component			
GLD409	109.80	1.92		−12.1	4.7	2.5	−7.3	2.0	3.5	0.4
GLD409	109.80	1.92	^{13}CO	−11.6	0.9'	2.2				0.1
GLD431	114.10	14.84		−4.0	5.7	2.4	−0.3	2.1	1.1	0.4
GLD433	114.30	−2.73		−3.1	2.7	2.1	−8.7	2.3	1.6	0.2
GLD439	115.80	−1.97		−2.5	4.3	4.2	−7.4	1.6	1.2	0.3
GLD439	115.80	−1.97	^{13}CO	−2.4	1.3	2.8				0.1
GLD447	117.10	12.40		3.5	5.4	1.8	−3.0	2.3	1.1	0.4
GLD447	117.10	12.40	^{13}CO	3.7	3.7	1.2				0.2
GLD459	120.70	−1.44		−19.5	3.9	3.3	−10.0	1.2	1.2	0.3
GLD459	120.70	−1.44	^{13}CO	−19.5	0.6	3.0				0.2
GLD467	121.90	−0.87		5.1	1.5	2.0	0.2	1.7	1.9	0.3
GLD472	122.20	−10.22		−10.7	4.2	1.2	−15.9	1.0	1.0	0.2
GLD472	122.20	−10.22	^{13}CO	−10.6	3.8	1.1				0.4
GLD479	125.40	−0.46		−13.5	2.2	2.9	−9.2	1.1	1.4	0.4
GLD479	125.40	−0.46	^{13}CO	−13.7	1.2	1.3				0.2
GLD484	126.60	−0.71		−15.3	10.3	2.9	−12.0	4.1	4.0	0.4
GLD489	128.80	13.81		3.2	3.3	1.6	−2.7	2.9	2.7	0.4
GLD489	128.80	13.81	^{13}CO	3.4	2.3	1.4				0.2
GLD495	133.00	0.95		−40.2	2.1	8.6	−43.9	2.5	2.6	0.4
GLD496	133.50	8.58		−4.1	2.8	1.6	−13.9	2.3	1.2	0.3
GLD496	133.50	8.58	^{13}CO	−4.0	1.1	1.4				0.1
GLD497	133.60	1.07		−40.0	4.1	2.1	−43.0	5.0	4.7	0.2
GLD497	133.60	1.07	^{13}CO	−40.4	1.9	1.9	−43.6	1.2	2.4	0.1
GLD500	136.90	1.17		−41.2	8.6	3.8	−37.2	3.3	2.2	0.3
GLD500	136.90	1.17	^{13}CO	−41.3	3.7	3.0	−37.3	1.2	1.7	0.1
GLD505	140.30	2.27		−13.2	4.0	2.4	−10.6	2.5	1.6	0.3
GLD505	140.30	2.27	^{13}CO	−13.4	1.3	2.4				0.2

Source	lII	bII		V_{12}	$T_a^\star$	ΔV	V_{12}	$T_a^\star$	ΔV	rms
				1^{st} component			2^{nd} component			
GLD514	143.50	1.51		−9.9	3.8	1.8	−0.1	1.5	2.3	0.3
GLD514	143.50	1.51	^{13}CO	−9.7	1.9	1.1				0.3
GLD518	148.70	2.11	^{13}CO	1.7	1.5	1.7	−3.0	1.4	1.2	0.2
GLD519	148.80	2.73		2.2	3.4	1.7	−3.2	2.2	2.0	0.3
GLD519	148.80	2.73	^{13}CO	2.1	1.3	1.4				0.1
GLD520	149.20	3.04		3.0	4.1	1.8	−3.9	3.9	1.7	0.2
GLD520	149.20	3.04	^{13}CO	3.1	2.8	1.4				0.1
GLD521	149.30	2.72		1.9	4.2	2.4	−4.0	3.0	1.3	0.2
GLD521	149.30	2.72	^{13}CO	1.8	1.1	2.4	−4.2	0.7	1.5	0.2
GLD524	149.90	2.74		3.6	3.1	1.1	1.4	1.4	1.6	0.3
GLD526	150.80	4.14		3.1	5.0	1.2	−6.9	2.9	1.4	0.4
GLD528	151.10	4.47		3.2	4.1	1.8	−6.8	1.8	1.1	0.3
GLD528	151.10	4.47	^{13}CO	2.9	2.5	1.1				0.1
GLD538	152.60	5.31		−5.9	5.3	1.8	−0.3	1.1	1.5	0.3
GLD538	152.60	5.31	^{13}CO	−5.9	3.1	1.4				0.2
GLD539	154.00	5.10		3.4	4.6	2.4	−1.4	1.0	3.0	0.3
GLD546	155.30	4.88		4.5	4.9	2.1	1.4	0.8	3.9	0.2
GLD550	155.90	5.28		5.2	4.4	2.0	2.3	3.3	2.3	0.3
GLD554	157.20	−8.72		−6.9	4.4	2.0	−9.1	1.6	1.8	0.1
GLD554	157.20	−8.72	^{13}CO	−7.3	2.1	1.8				0.1
GLD555	157.30	−1.10		4.9	6.0	0.7	−8.3	2.5	2.6	0.2
GLD556	157.70	−8.86		−5.8	3.7	1.5	−7.7	0.8	4.9	0.1
GLD557	157.90	−8.66		−5.1	4.0	2.0	−7.5	2.3	3.3	0.1
GLD557	157.90	−8.66	^{13}CO	−5.1	2.7	1.5	−6.9	0.7	3.1	0.2
GLD558	157.90	−8.95		−5.5	5.6	1.8	−8.9	0.4	4.2	0.2
GLD558	157.90	−8.95	^{13}CO	−5.5	2.6	1.3				0.2
GLD560	159.60	11.35		2.5	4.1	1.5	−3.8	0.7	1.9	0.2
GLD569	167.30	−4.24		5.0	2.5	3.5	−1.4	1.4	1.2	0.1

Source	lII	bII		V	$T_a^\star$	ΔV	V_{12}	$T_a^\star$	AV	rms
				1st component			2nd component			
GLD585	172.40	−8.11		5.4	4.8	1.2	7.8	1.4	1.8	0.2
GLD589	173.00	−5.48		6.8	4.4	1.1	−4.2	1.1	1.8	0.1
GLD589	173.00	−5.48	^{13}CO	6.5	1.8	0.9				0.2
GLD590	173.40	−13.76		6.2	4.0	2.7	4.6	2.5	1.1	0.2
GLD590	173.40	−13.76	^{13}CO	6.1	3.0	1.4				0.2
GLD610	180.80	4.40		1.6	2.4	3.2	3.6	1.8	1.6	0.1
GLD610	180.80	4.40	^{13}CO	2.5	2.1	2.0				0.3
GLD619	195.10	−16.91	^{13}CO	−2.3	3.0	1.4	−0.7	0.8	1.4	0.1
GLD623	204.40	−11.20		1.0	6.1	1.4	9.2	2.1	2.8	0.2
GLD624	204.40	−11.30		0.7	4.7	1.6	9.8	2.4	2.3	0.1
GLD625	204.50	−10.96		1.1	2.6	0.8	10.1	1.2	2.2	0.2
GLD626	204.70	−11.71		0.8	7.3	2.1	10.4	3.1	2.3	0.1
GLD627	204.80	−11.48		1.0	4.7	1.5	10.3	1.5	2.9	0.2
GLD632	207.30	−16.46		9.6	4.9	3.9	5.3	1.0	2.6	0.2
GLD633	207.40	−1.22		10.3	3.0	2.4	4.3	2.8	2.0	0.1
GLD633	207.40	−1.22	^{13}CO	10.7	0.5	1.5	4.2	0.6	0.9	0.1
GLD637	208.40	−18.71		6.7	1.5	2.3	13.5	4.4	1.9	0.3
GLD643	212.50	−19.00		2.7	15.6	1.9	5.6	6.8	1.9	0.2
GLD643	212.50	−19.00	^{13}CO	3.0	5.0	1.7	5.7	2.9	1.2	0.1
GLD644	212.90	−19.38		5.3	4.5	2.1	2.8	4.2	2.5	0.1
GLD645	212.90	−12.44		12.6	5.1	3.5				0.2
GLD645	212.90	−12.44	^{13}CO	12.7	1.2	2.6	16.9	0.8	0.9	0.2
GLD648	215.70	−12.89		5.6	3.9	1.7	11.2	1.6	3.3	0.2
GLD652	223.50	−1.79		18.5	6.4	2.2	16.5	2.3	2.1	0.2
GLD652	223.50	−1.79	^{13}CO	18.4	2.9	1.7				0.2
GLD655	225.00	−2.73		10.4	6.2	2.2	14.7	3.9	1.8	0.2
GLD655	225.00	−2.73	^{13}CO	10.8	1.3	1.6	14.5	0.8	1.1	0.1
GLD659	237.40	−4.74		19.5	6.3	2.1	21.6	3.4	1.5	0.2
GLD660	238.40	−4.14		19.7	5.9	2.4	17.2	3.7	2.0	0.1

Source	lII	bII		V_{12}	$T_a^\star$	ΔV	V_{12}	$T_a^\star$	ΔV	V_{12}	$T_a^\star$	ΔV	rms
				1^{st} component			2^{nd} component			3^{rd} component			
GLD152	28.84	−1.74		10.7	3.5	1.5	3.0	3.4	1.2	4.7	2.9	2.0	0.3
GLD152	28.84	−1.74	^{13}CO	10.7	1.6	1.3	3.9	1.3	1.8				0.1
GLD226	55.35	3.06		8.3	3.0	2.3	6.7	2.6	1.0	2.5	1.7	2.4	0.2
GLD226	55.35	3.06	^{13}CO	7.1	1.0	1.8							0.1
GLD291	77.74	0.81		3.2	4.1	5.5	6.7	2.4	1.8	0.7	2.0	2.2	0.3
GLD291	77.74	0.81	^{13}CO	2.0	2.3	2.3	6.8	0.9	1.3				0.2
GLD292	77.80	0.84		1.3	4.7	4.6	6.3	2.1	3.1	9.8	1.3	1.4	0.2
GLD292	77.80	0.84	^{13}CO	1.7	3.0	3.0							0.1
GLD306	85.07	−0.16		1.1	4.1	3.9	−4.5	11.4	3.2	−5.8	2.7	1.0	0.3
GLD306	85.07	−0.16	^{13}CO	0.8	1.5	1.7	−4.8	6.6	2.1				0.2
GLD307	85.12	0.38		−3.0	5.4	3.1	0.0	2.2	2.5	2.4	2.4	1.3	0.3
GLD307	85.12	0.38	^{13}CO	−2.4	3.1	2.1	0.2	0.6	2.0				0.2
GLD314	86.42	0.18		0.7	2.8	2.7	−16.3	2.3	1.9	−13.9	1.9	2.6	0.2
GLD548	155.50	−14.58		2.1	2.1	2.6	0.1	3.0	1.8	−3.0	0.6	4.8	0.1
GLD548	255.50	−14.58	^{13}CO	1.9	3.7	1.5	0.3	0.6	1.5				0.2
GLD591	173.50	2.88		−21.4	3.8	5.2	−11.8	1.2	2.1	−23.1	0.7	1.0	0.2
GLD631	206.50	−16.33		11.2	19.9	2.9	8.7	12.8	2.1	4.8	4.5	2.6	0.3

SOUTHERN CLOUDS

Source	lII	bII	V_{12}	$T^{\star}_{a,12}$	ΔV_{12}	rms	V_{13}	$T^{\star}_{a,13}$	ΔV_{13}	rms
SDC002	237.40	−2.89					25.4	0.7	1.2	0.1
SDC004	237.40	−4.86	20.7	6.1	2.3	0.2	20.6	1.0	2.5	0.1
SDC009	239.40	−4.70	23.4	7.1	3.3	0.2	23.6	3.8	2.2	0.2
SDC012	247.00	−0.61	20.9	1.3	4.2	0.3				
SDC013	247.30	−2.79	−23.4	1.3	1.5	0.2				
SDC018	250.30	0.25	12.5	2.1	2.2	0.2				
SDC024	253.10	−4.28	11.4	5.4	1.4	0.4				
SDC025	253.10	−1.37	10.4	2.9	1.1	0.4				
SDC026	253.30	3.30	6.7	2.1	1.6	0.2				
SDC030	255.40	−4.88					9.3	3.5	1.0	0.2
SDC031	255.50	−4.20	9.8	2.4	1.5	0.2				
SDC032	255.80	−2.71	9.4	7.4	2.2	0.2				
SDC036	258.10	−3.15	−20.4	1.6	0.7	0.3				
SDC040	259.00	0.96	6.0	2.1	3.6	0.2				
SDC041	259.20	3.35	6.9	2.5	2.7	0.4				
SDC042	259.30	−13.26	4.8	8.2	1.3	0.6				
SDC044	259.50	−16.54	−21.4	2.5	1.5	0.3				
SDC046	259.80	−2.59	9.1	3.4	1.7	0.6				
SDC049	260.60	−3.63	6.2	3.7	1.6	0.3	6.2	1.1	0.9	0.2
SDC050	260.60	−3.70	5.5	3.0	2.7	0.6				
SDC055	262.20	−12.46	5.2	4.4	2.0	0.2				
SDC056	262.40	3.12	9.0	2.1	2.4	0.3				
SDC058	263.10	1.35	6.3	3.1	2.2	0.2	6.4	1.3	1.8	0.3
SDC071	265.90	−7.53	3.3	7.7	1.5	0.7	3.5	1.5	1.2	0.2
SDC072	266.00	−7.63	3.3	7.8	1.8	0.3	3.5	1.5	1.3	0.3
SDC075	266.70	4.93	2.6	2.4	2.7	0.4	2.7	1.3	1.3	0.2
SDC080	267.30	0.04	4.8	4.7	4.2	0.5				
SDC081	267.50	4.30	1.0	2.5	3.4	0.3	0.4	1.5	2.5	0.3

Source	lII	bII	V_{12}	$T^{\star}_{a,12}$	ΔV_{12}	rms	V_{13}	$T^{\star}_{a,13}$	ΔV_{13}	rms
SDC082	267.60	−7.35	5.4	4.5	2.1	0.5				
SDC085	268.10	1.82	−0.5	3.6	3.6	0.3	−0.2	2.1	1.7	0.3
SDC087	268.50	−1.74					1.7	0.8	4.5	0.3
SDC091	269.40	−7.57	4.8	3.6	1.2	0.7				
SDC093	269.80	4.02	−3.0	4.4	1.8	0.6	21.1	1.0	0.7	0.3
SDC094	269.80	−11.10	0.1	4.8	1.6	0.6				
SDC096	270.00	2.88	−2.7	3.2	4.9	0.3	−2.2	1.6	3.5	0.2
SDC098	270.10	−0.28	1.2	4.2	4.2	0.6	0.8	2.4	2.9	0.1
SDC101	270.50	−1.75	4.7	3.8	5.2	0.8				
SDC105	270.90	2.48	−3.5	1.9	2.6	0.6				
SDC109	271.40	4.89	−3.2	4.4	5.1	0.2	−3.2	2.7	2.7	0.2
SDC111	272.50	−3.93	5.4	3.0	2.0	0.4				
SDC111A	275.30	−1.11	−4.8	2.6	1.9	0.7				
SDC114	274.60	0.13	−2.2	4.2	4.9	0.4				
SDC116	275.50	2.14	−6.2	2.6	5.5	0.6	−6.5	0.8	2.4	0.2
SDC118	276.30	−0.68	−3.9	2.9	1.0	0.5	−7.7	0.8	2.9	0.3
SDC142	285.20	9.44	5.7	1.8	1.3	0.2	15.6	1.7	1.3	0.5
SDC152	287.80	7.66	4.7	2.4	1.2	0.5				
SDC152A	287.80	7.67	10.9	3.0	3.1	0.6				
SDC163	291.00	7.82	8.2	1.7	1.6	0.6				0.3
SDC163A	291.10	7.85	6.3	2.7	3.6	0.6	−8.8	1.4	1.4	
SDC206	301.70	7.63	13.5	2.2	2.0	0.5				
SDC228	304.00	7.37	14.5	4.4	0.9	0.7				
SDC243	307.10	6.54	−13.7	3.2	2.3	0.2	−12.7	2.0	1.5	0.2
SDC249	308.40	5.81					−2.3	1.0	1.4	0.3
SDC259	311.10	5.79	18.2	1.0	3.9	0.3	−23.6	3.0	1.3	0.7
SDC262	311.60	−1.18	−1.8	6.1	1.6	1.4				
SDC277	315.90	5.90	6.0	4.0	1.5	0.4	6.7	1.1	2.1	0.3
SDC278	316.10	4.94	−3.1	6.6	2.4	0.5				
SDC293	319.70	1.53	−17.3	5.7	2.3	0.6				

Source	lII	bII	V_{12}	$T^{\star}_{a,12}$	ΔV_{12}	rms	V_{13}	$T^{\star}_{a,13}$	ΔV_{13}	rms
SDC302	323.10	−0.96	−6.0	3.9	2.5	0.6				
SDC305	323.80	5.59	−20.2	4.3	1.9	0.3				
SDC311	326.30	−0.58	−17.3	2.6	4.0	0.9				
SDC316	331.80	1.82	27.3	2.5	1.0	0.4				
SDC320	334.30	−1.01	−11.3	3.7	3.6	0.4				
SDC321	334.60	18.09	5.8	6.6	1.8	0.2	5.4	1.0	4.7	0.4
SDC328	335.40	−1.14	−11.8	2.3	4.9	0.3				
SDC332	336.10	−2.31	−12.1	1.2	1.1	0.6				
SDC333	336.30	3.94					31.5	2.2	1.2	0.6
SDC334	336.40	11.31	6.5	1.9	2.7	0.3				
SDC336	336.50	19.14	6.0	3.7	1.9	0.3				
SDC337	336.80	−0.96	−21.8	9.0	2.5	0.3				
SDC339	337.00	4.84	4.1	8.9	2.0	0.5				
SDC341	337.40	16.68					5.0	0.6	1.7	0.2
SDC348	338.90	9.50					6.1	2.4	0.9	0.1
SDC349	339.00	16.16					4.9	3.7	1.3	0.1
SDC365	342.10	−3.72					−15.7	4.3	2.6	0.2
SDC383	346.70	−9.72	4.9	2.7	1.7	0.5				
SDC392	347.90	3.16	−2.9	2.9	1.5	0.3				
SDC395	348.80	3.57	2.2	2.3	3.0	0.3				
SDC398	350.6	2.6	6.1	3.5	2.6	0.2				
SDC403	352.00	16.31	3.9	1.1	1.8	0.3				
SDC406	352.60	1.02	5.5	4.5	1.8	0.5	5.5	2.1	1.1	0.4
SDC408	352.80	17.85	2.8	1.9	2.2	0.3				
SDC411	353.60	15.78	4.0	13.5	2.0	0.2				
SDC414	354.30	16.35	2.2	8.0	1.6	0.2				
SDC415	354.5	−1.7	3.4	1.5	4.3	0.2				
SDC418	354.90	14.97	3.4	12.1	1.6	0.2				
SDC419	354.90	16.00	2.5	5.9	1.4	0.3				
SDC429	357.2	4.4	6.4	3.0	2.0	0.3				

Source	lII	bII	V_{12}	$T^{\star}_{a,12}$	A	rme	V_{13}	$T^{\star}_{a,13}$	ΔV_{13}	rms
SDC431	357.3	0.9	1.7	1.9	3.7	0.4				
SDC439	358.60	15.37	2.5	7.1	1.9	0.3				
SDC441	358.9	–3.9	5.2	2.7	2.9	0.4				
SDC446	359.80	–18.31	5.3	9.3	2.1	0.3				
SDC450	0.22	–18.73	4.7	6.1	1.7	0.2				
SDC453	1.07	–20.52	4.9	3.9	1.7	0.3				
SDC456	1.44	9.38	3.5	8.1	1.6	0.3				
SDC464	3.67	6.35	4.3	3.4	1.4	0.2				
SDC473	6.11	–1.22	13.4	1.9	10.1	0.2				
SDC476	6.69	–0.55	–102.5	0.9	2.8	0.3				
SDC477	6.84	–2.15	10.8	5.6	2.0	0.2				
SDC479	7.09	–2.32	9.4	0.8	4.1	0.2				

SOUTHERN CLOUDS WITH MULTIPLE COMPONENTS

Source	lII	bII		V_{12}	$T^{\star}_{a}$	AV	V_{12}	$T^{\star}_{a}$	AV	rms
				1st component			2nd component			
SDC006	**238.40**	**–4.12**		**20.5**	**4.5**	**2.2**	**18.9**	**3.8**	**3.4**	**0.2**
SDC006	**238.40**	**–4.12**	^{13}CO	**20.2**	**2.6**	**2.1**				**0.2**
SDC007	**238.90**	**–1.57**		**19.1**	**3.6**	**2.6**	**27.1**	**1.1**	**1.4**	**0.1**
SDC007	**238.90**	**–1.57**	^{13}CO	**19.1**	**1.0**	**1.3**				**0.2**
SDC022	**251.90**	**–3.16**		**18.3**	**1.4**	**1.2**	**13.1**	**2.9**	**2.9**	**0.1**
SDC038	**258.60**	**–2.69**		**17.8**	**1.3**	**3.6**	**9.5**	**2.7**	**3.1**	**0.2**
SDC052	**261.60**	**0.33**		**5.3**	**2.7**	**4.5**	**10.9**	**3.2**	**3.3**	**0.3**
SDC053	**261.70**	**–4.36**		**10.0**	**2.8**	**5.5**	**13.5**	**1.3**	**1.3**	**0.3**
SDC064	**265.10**	**1.43**		**5.2**	**8.1**	**2.7**	**8.1**	**5.9**	**2.7**	**0.3**
SDC064	**265.10**	**1.43**	^{13}CO	**6.3**	**4.1**	**2.9**				**0.1**
SDC067	**265.40**	**0.41**		**0.0**	**2.0**	**1.8**	**5.9**	**4.3**	**3.2**	**0.5**
SDC078	**267.00**	**–0.94**		**4.4**	**4.3**	**3.7**	**7.7**	**2.5**	**2.2**	**0.4**

Source	*lII*	*bII*		V_{12}	$T_a^\star$	ΔV	V_{12}	$T_a^\star$	ΔV	rms
				1st component			2nd component			
SDCOSO	269.40	−1.34		4.0	5.8	3.9	8.2	2.3	2.2	0.6
SDCOSO	269.40	−1.34	^{13}CO	4.0	2.3	2.3				0.2
SDC099	270.20	−0.98		6.1	3.7	2.5	0.6	4.2	2.6	0.9
SDC102	270.50	0.53		−0.2	4.1	3.8	6.6	5.1	3.6	0.4
SDC122	277.10	−2.56		−6.7	4.0	0.7	−2.0	2.5	3.6	0.6
SDC145	286.20	0.10		−20.0	6.5	3.5	−8.6	1.9	3.2	0.2
SDC145	286.20	0.10	^{13}CO	−20.3	1.9	2.6				0.2
SDC149	287.20	−0.21		−18.5	7.0	3.9	−7.6	1.0	2.3	0.2
SDC149	287.20	−0.21	^{13}CO	−18.2	3.2	2.1				0.3
SDC327	335.30	3.15	^{13}CO	7.4	0.6	2.2	3.4	2.0	1.6	0.2
SDC342	338.00	16.58		5.2	9.9	1.6	6.8	3.6	1.6	0.2
SDC342	338.00	16.58	^{13}CO	5.4	3.2	2.2				0.2
SDC372	344.00	−0.41	^{13}CO	33.7	1.5	0.9	37.0	1.7	1.2	0.3
SDC388	347.00	0.51		−9.8	3.8	3.4	6.1	6.5	1.1	0.4
SDC388	347.00	0.51	^{13}CO	−9.4	0.8	4.1				0.1
SDC400	350.80	1.0		5.7	2.9	1.9	−5.4	1.2	2.8	0.3
SDC406	352.60	1.0		5.5	3.6	1.9	−1.1	1.2	5.1	0.2
SDC409	352.90	16.93		2.4	10.6	1.0	3.2	13.0	2.4	0.2
SDC421	355.10	1.6		7.1	4.3	2.4	−1.9	0.8	2.2	0.3
SDC435	357.90	−2.0		−0.5	3.5	4.9	4.3	3.3	3.4	0.4
SDC445	359.60	−17.75		3.6	1.7	1.2	6.1	5.4	2.3	0.3
SDC449	0.21	−4.52		5.7	1.6	1.8	8.7	2.3	3.2	0.2

Source	*lII*	*bII*		V_{12}	$T_a^\star$	ΔV	V_{12}	$T_a^\star$	AV	V_{12}	$T_a^\star$	AV	rms
				1st component			2nd component			3rd component			
SDC134	281.60	−0.81		−3.4	3.8	6.4	3.8	2.2	3.4	−11.8	1.3	1.9	0.2
SDC134	281.60	−0.81	^{13}CO	−4.2	1.6	1.9							0.2
SDC407	352.70	0.9		2.6	4.8	2.9	5.7	2.7	1.8	−1.9	1.0	3.4	0.3

CLOUDS WITH ASSOCIATED REFLECTION NEBULAE

Source	lII	bII	V_{12}	$T^{\star}_{a,12}$	ΔV_{12}	rms	V_{13}	$T^{\star}_{a,13}$	ΔV_{13}	rms
GGR007	123.60	−1.69	−20.9	0.9	2.9	0.2				
GGR033	203.50	−24.70	7.4	11.1	2.5	0.2				
GGR052	208.70	−20.40	10.9	5.0	2.0	0.7				
GGR099	355.50	20.90	3.1	5.1	1.0	0.3				
GGR101	355.50	20.80	2.9	6.7	1.1	0.2				
GGR107	0.80	18.40	6.2	2.5	1.2	0.3				
GGR144	111.60	13.70	−3.7	2.1	1.2	0.5				
RN14	172.10	−9.71	6.6	2.6	2.8	0.1	6.1	1.4	4.8	0.4
RN36	355.20	20.95					3.0	1.0	2.3	0.2
RN39	352.90	17.04					3.0	1.8	1.7	0.1
VDB156A	103.20	−15.25	3.5	2.2	1.9	0.1				
VDB156B	103.10	−17.09	−8.7	1.8	1.0	0.2				
VDB156C	100.80	−16.55	−5.7	1.2	1.1	0.2				
VDB156D	101.00	−15.54	−9.2	1.2	1.4	0.1				

REFLECTION NEBULAE WITH MULTIPLE COMPONENTS

Source	lII	bII		V_{12}	$T^{\star}_{a}$	ΔV	V_{12}	$T^{\star}_{a}$	ΔV	rms
				1^{st} component			2^{nd} component			
GGR041	208.80	−20.40		7.3	0.5	1.7	10.2	5.2	1.5	0.2
RN16	172.50	−7.98		5.7	6.8	0.9				0.1
RN16	172.50	−7.98	^{13}CO	5.7	4.0	1.1	3.0	0.8	2.7	0.4
VDB018	155.50	−14.56		2.2	2.1	2.3	−0.0	2.1	1.5	0.2

Appendix *C*

Plots of a sample of 48 interesting spectra selected on the basis of their line strengths, line widths or shapes of the line profiles are given in this Appendix. In all cases, the horizontal axis is the LSR velocity and the vertical axis is the calibrated antenna temperature T_a^*. Date and frequency of observation and the source name are given at the bottom of each plot. A peak position on the spectral lines are marked with a + symbol. The three numbers written along with it are the channel number, the velocity, and the line strength at the marked position.

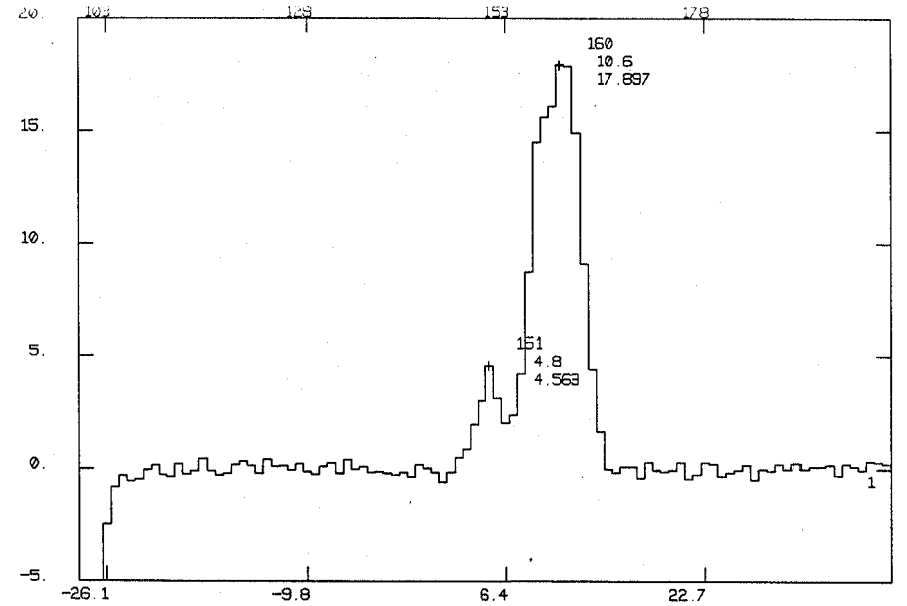
20.
15.
10.
5.
0.
-5.
103
128
153
178
160
10.6
17.897
151
4.8
4.563
1
-26.1
-9.8
6.4
22.7
DATE 4- 2-92 IST =22:15 FREQ=115271.20 SYN= 103.451 FB=0.2500 SB=3
SCAN = 1 GLD631

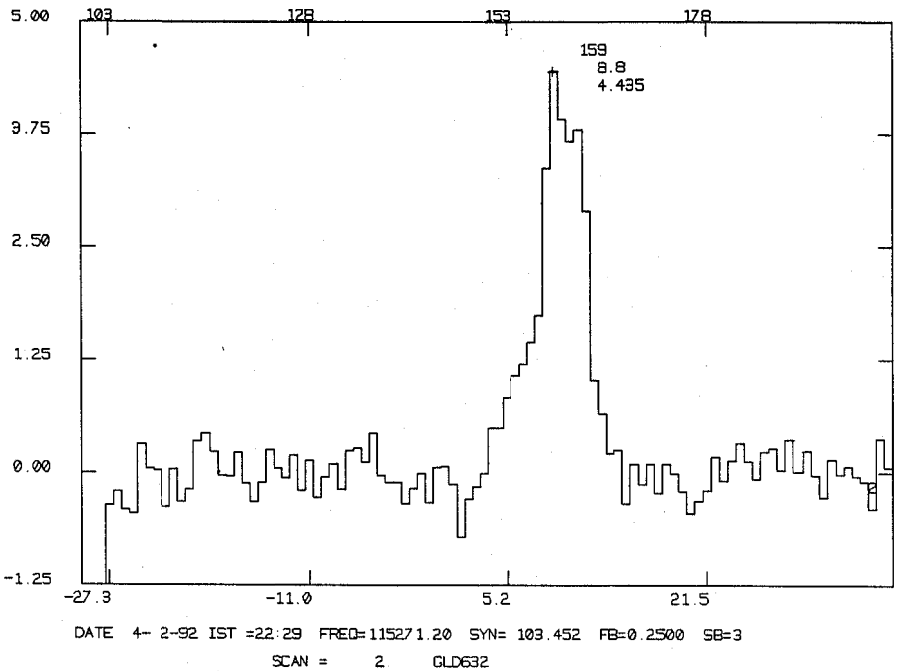
5.00
3.75
2.50
1.25
0.00
-1.25
103
128
153
178
159
8.8
4.435
-27.3
-11.0
5.2
21.5
DATE 4- 2-92 IST =22:29 FREQ=115271.20 SYN= 103.452 FB=0.2500 SB=3
SCAN = 2 GLD632

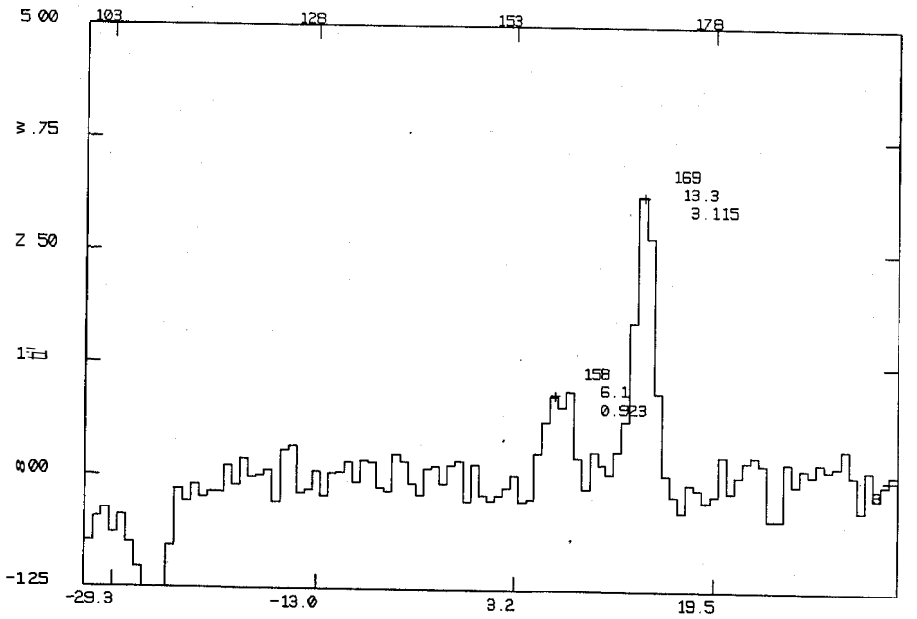
5 00
3.75
Z 50
1
0.00
-1.25
103
128
153
178
169
13.3
3.115
158
6.1
0.923
-29.3
-13.0
3.2
19.5
DATE 4- 2-92 IST =23:21 FREQ=115271.20 SYN= 103.452 FB=0.2500 SB=3
SCAN = 3 GLD637

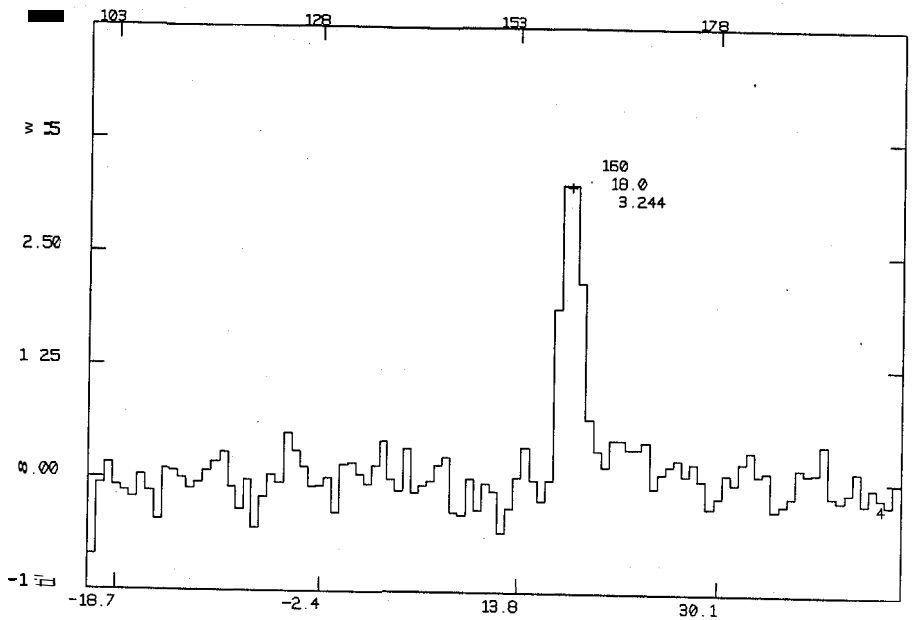
3.75
2.50
1.25
0.00
-1
103
128
153
178
160
18.0
3.244
-18.7
-2.4
13.8
30.1
DATE 4- 2-92 IST =23:38 FREQ=115271.20 SYN= 103.454 FB=0.2500 SB=3
SCAN = 4 GLD662

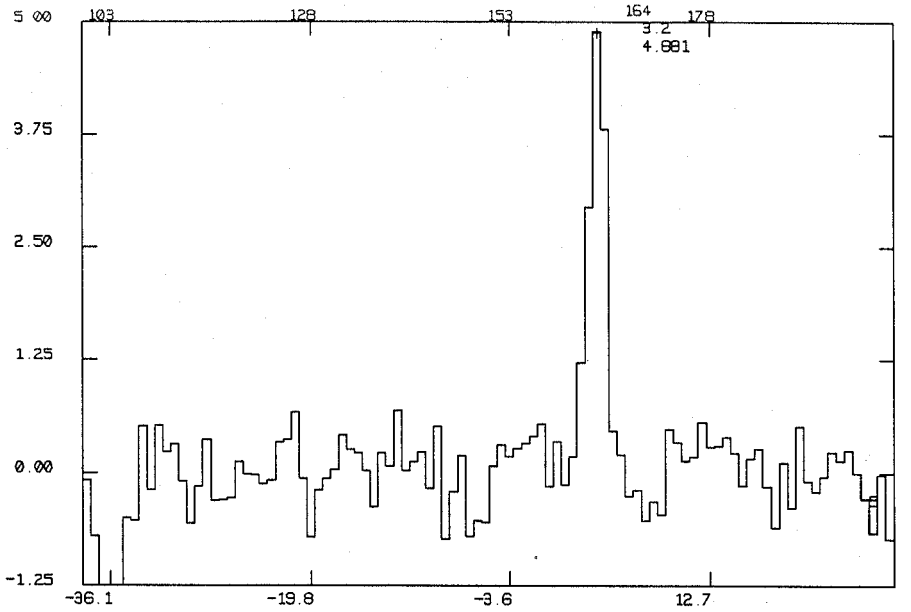

DATE 4- 2-92 IST =23:55 FREQ=11527 1.20 SYN= 103.464. FB=0.2500 SB=3

SCAN = 5 SDC072

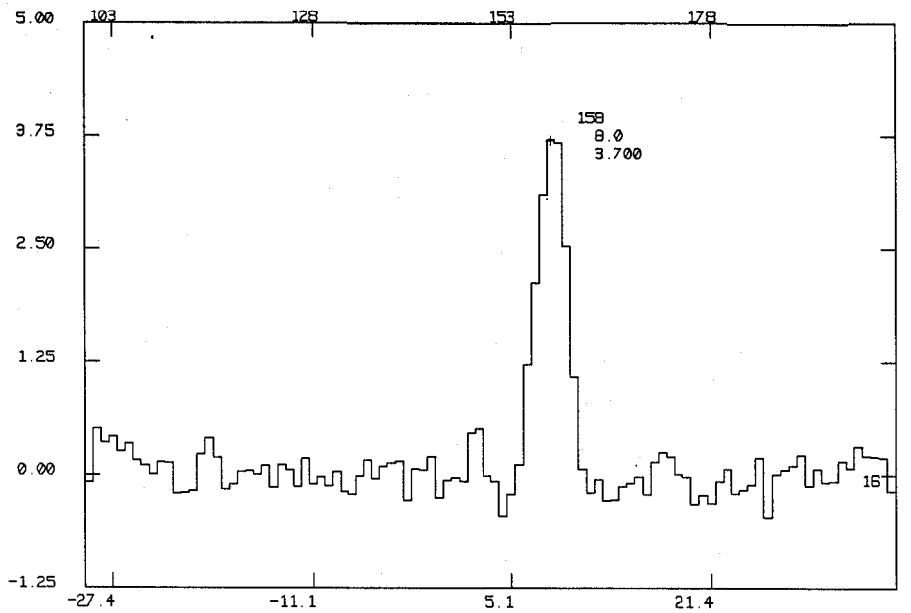

DATE 5- 2-92 IST =14:11 FREQ=11527 1.20 SYN= 103.466 FB=0.2500 SB=3

SCAN = 16 GLD353

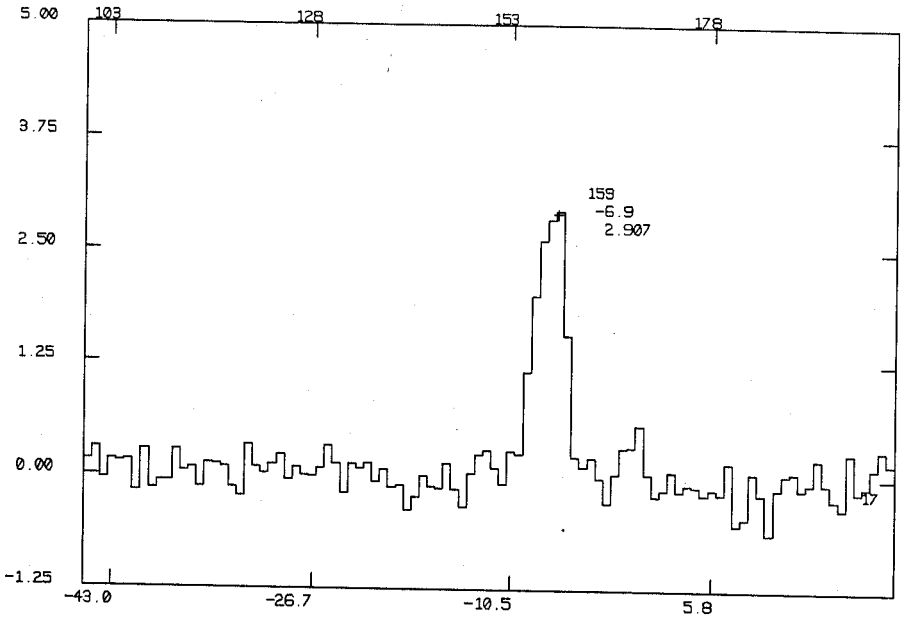
5.00
3.75
2.50
1.25
0.00
-1.25
103
128
153
178
159
-6.9
2.907
17
-43.0
-26.7
-10.5
5.8
DATE 5- 2-92 IST =14:34 FREQ=115271.20 SYN= 103.470 FB=0.2500 SB=3
SCAN = 17 GLD385

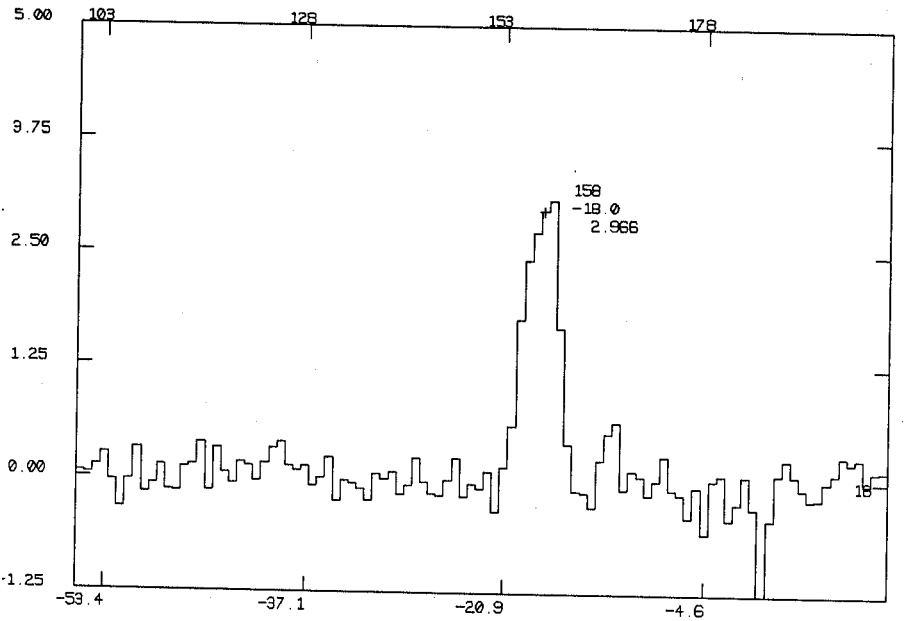
5.00
3.75
2.50
1.25
0.00
-1.25
103
128
153
178
158
-18.0
2.966
18
-53.4
-37.1
-20.9
-4.6
DATE 5- 2-92 IST =16: 7 FREQ=115271.20 SYN= 103.470 FB=0.2500 SB=3
SCAN = 18 GLD460

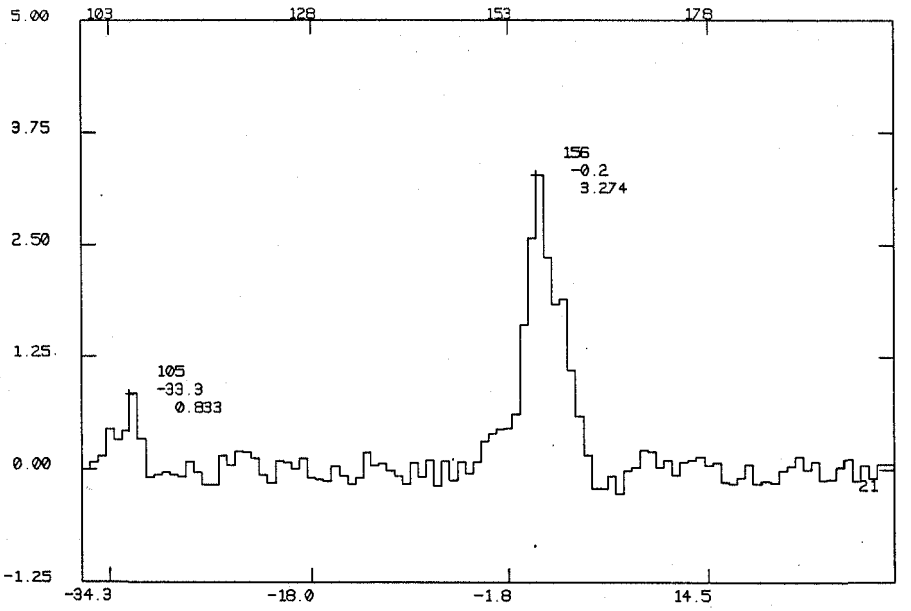

DATE 5- 2-92 IST =17:48 FREQ=11527 1.20 SYN= 103.456 FB=0.2500 SB=3

SCAN = 21 GLD548

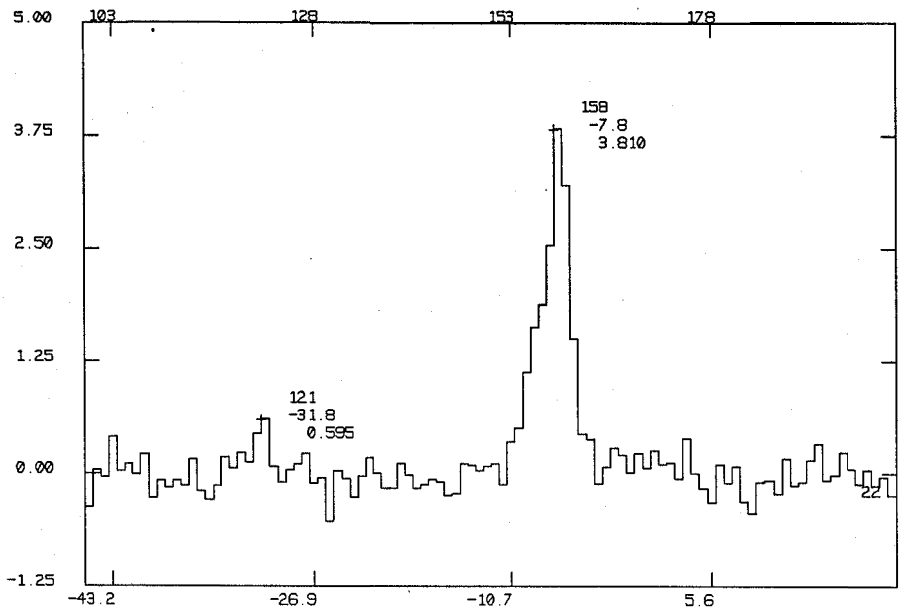

DATE 5- 2-92 IST =18:21 FREQ=11527 1.20 SYN= 103.460 FB=0.2500 SB=3

SCAN = 22 GLD554

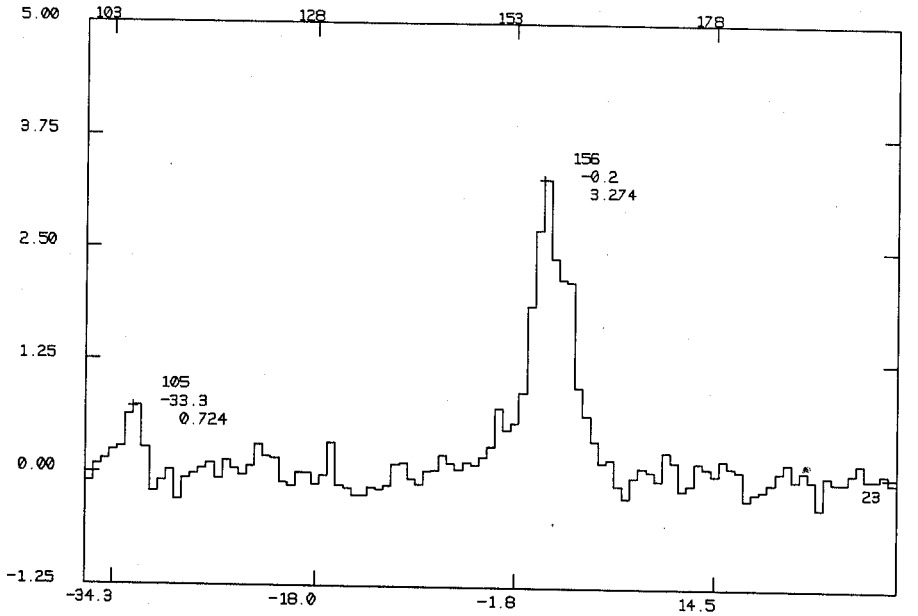

DATE 5- 2-92 IST =18:52 FREQ=11527 1.20 SYN= 103.456 FB=0.2500 SB=3

SCAN = 23 GLD548

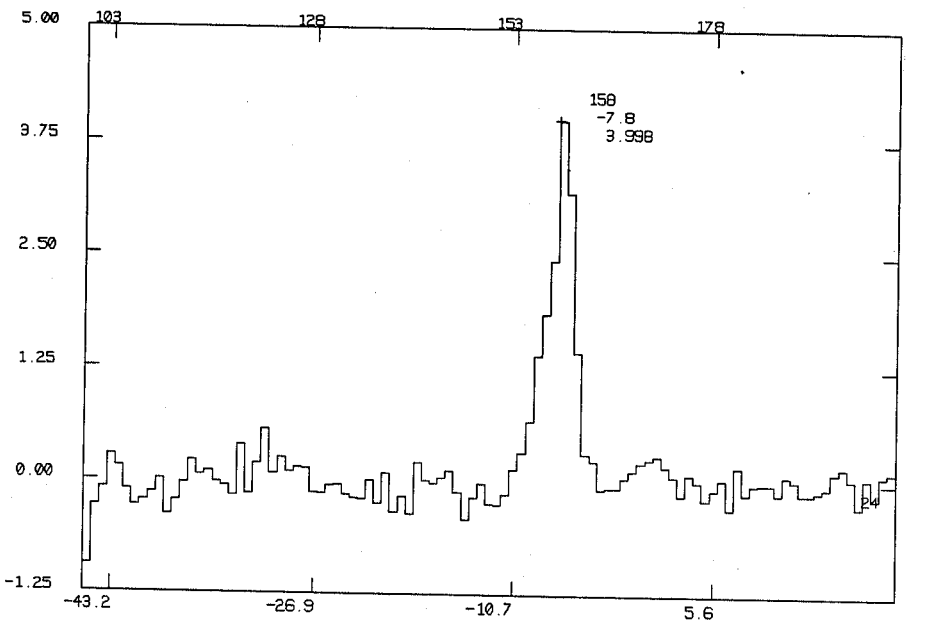

DATE 5- 2-92 IST =19: 9 FREQ=11527 1.20 SYN= 103.460 FB=0.2500 SB=3

SCAN = 24 GLD554

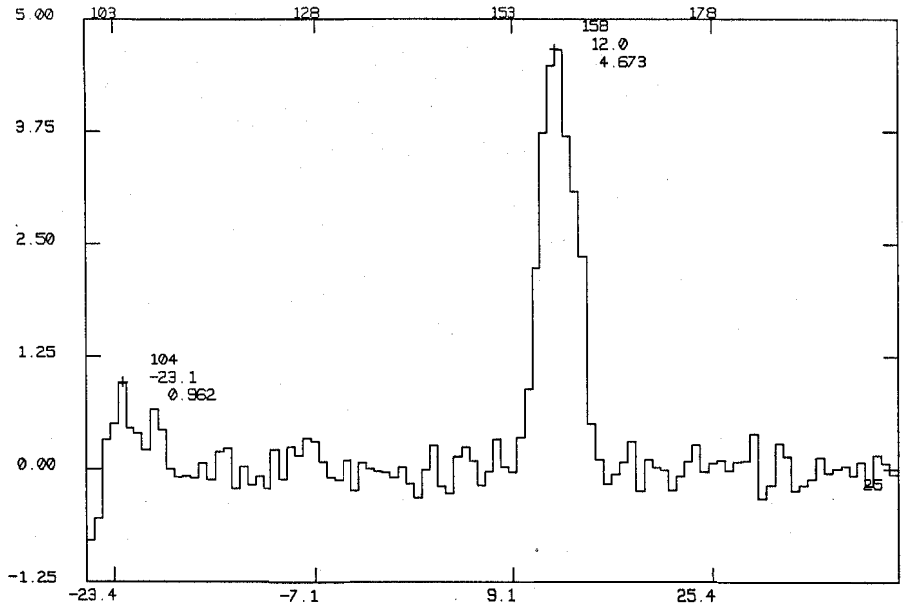
5.00
3.75
2.50
1.25
0.00
-1.25
103
128
153
178
158
12.0
4.673
104
-23.1
0.962
25
-23.4
-7.1
9.1
25.4
DATE 5- 2-92 IST =21:12 FREQ=115271.20 SYN= 103.451 FB=0.2500 SB=3
SCAN = 25 GLD645

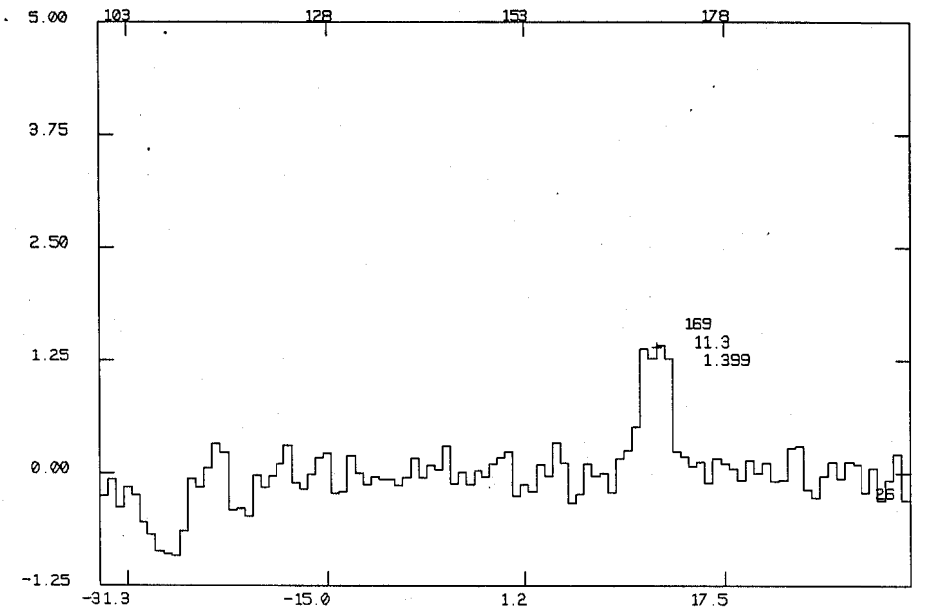
5.00
3.75
2.50
1.25
0.00
-1.25
103
128
153
178
169
11.3
1.399
25
-31.3
-15.0
1.2
17.5
DATE 5- 2-92 IST =21:30 FREQ=115271.20 SYN= 103.455 FB=0.2500 SB=3
SCAN = 26 GLD651

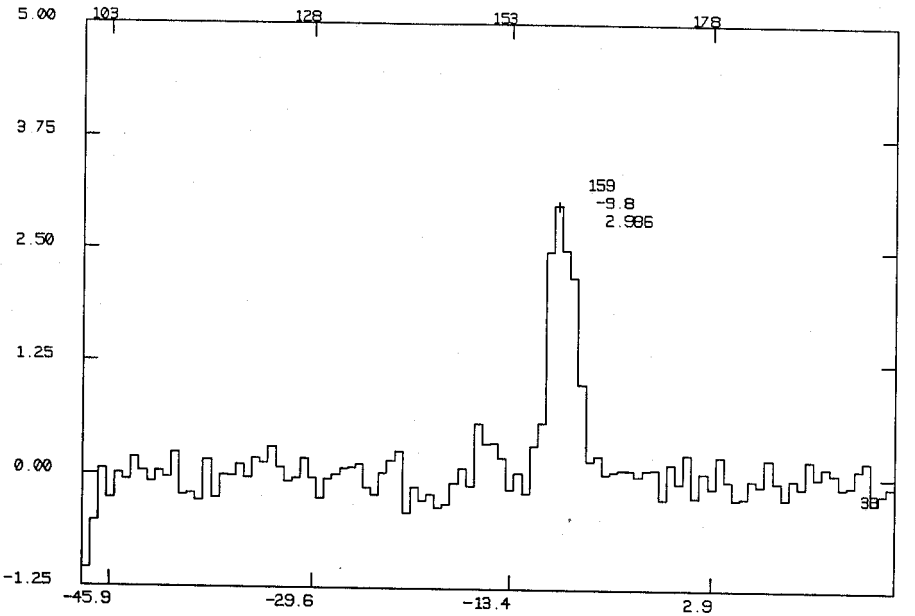
5.00
3.75
2.50
1.25
0.00
-1.25
103
128
153
178
159
-9.8
2.986
-45.9
-29.6
-13.4
2.9
DATE 6- 2-92 IST =16:17 FREQ=115271.20 SYN= 103.466 FB=0.2500 SB=3
SCAN = 33 GLD466

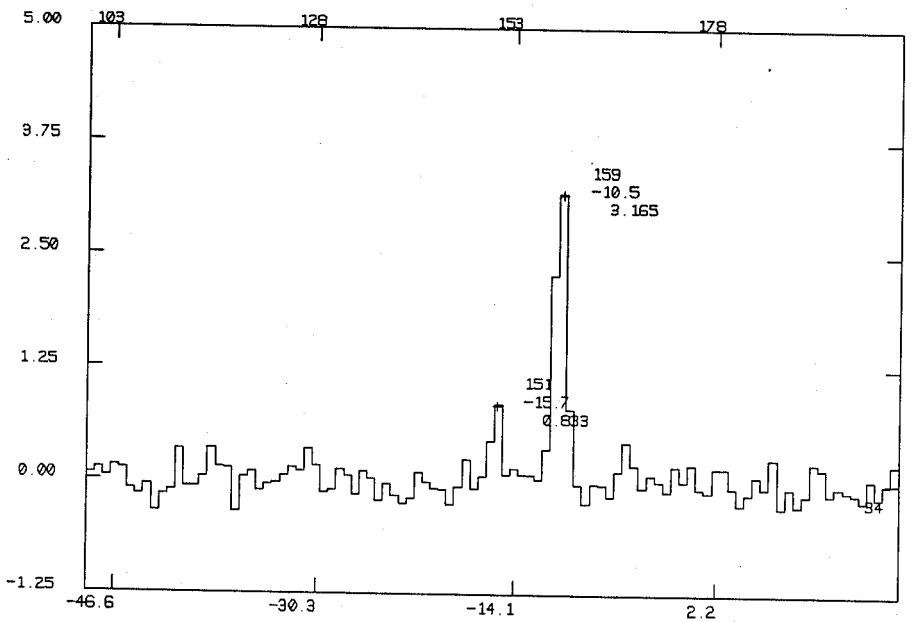
5.00
3.75
2.50
1.25
0.00
-1.25
103
128
153
178
159
-10.5
3.165
-46.6
-30.3
-14.1
2.2
DATE 6- 2-92 IST =16:31 FREQ=115271.20 SYN= 103.466 FB=0.2500 SB=3
SCAN = 34 GLD472

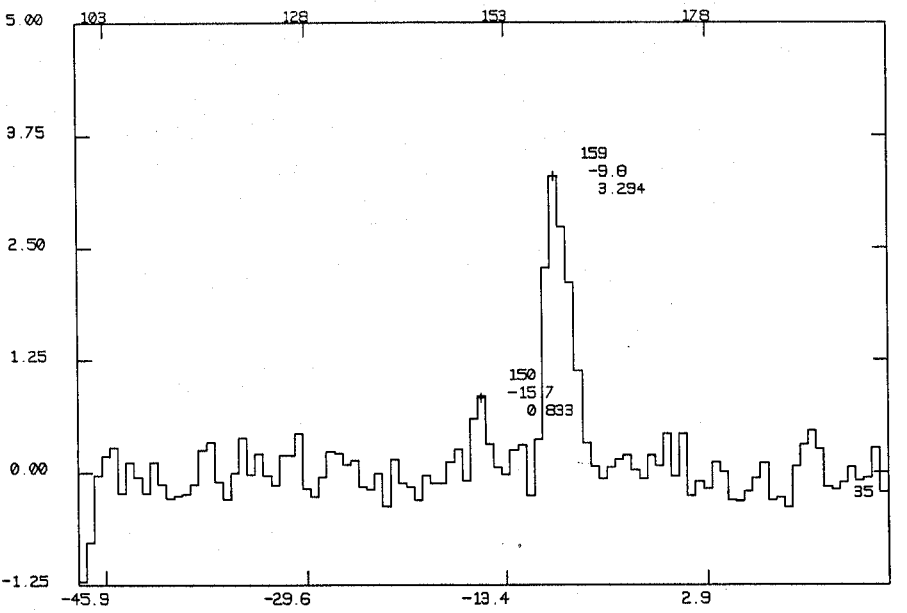

DATE 6- 2-92 IST =16:57 FREQ=11527.20 SYN= 103.466 FB=0.2500 SB=3

SCAN = 35 GLD466

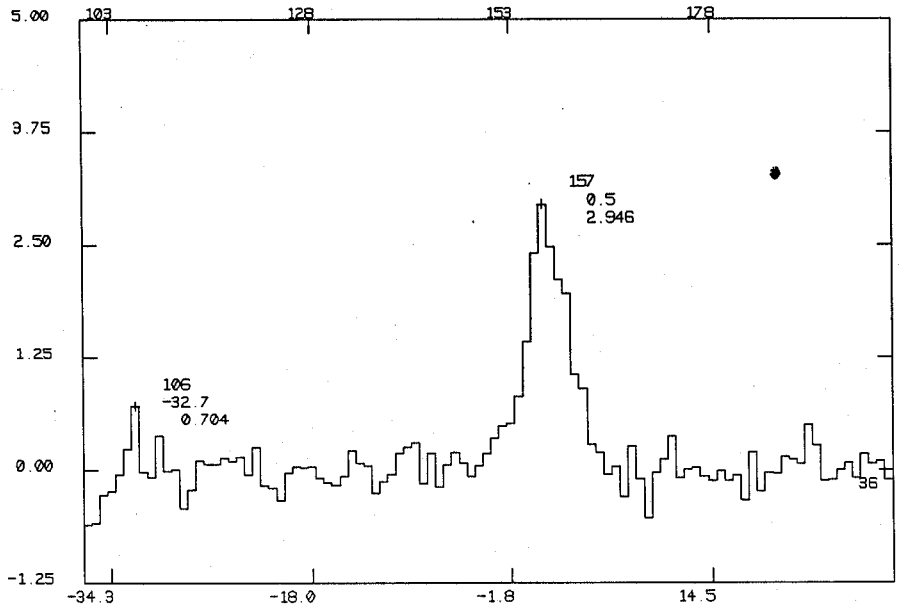

DATE 6- 2-92 IST =17:25 FREQ=11527.20 SYN= 103.456 FB=0.2500 SB=3

SCAN = 36 GLD548

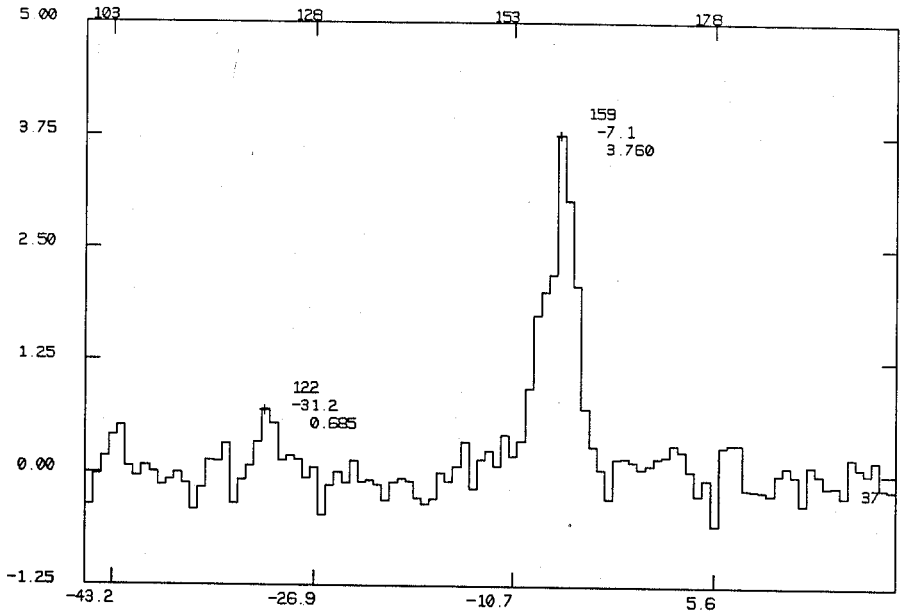
5.00
3.75
2.50
1.25
0.00
-1.25
103
128
153
178
159
-7.1
3.760
122
-31.2
0.685
-43.2
-26.9
-10.7
5.6
37
DATE 6- 2-92 IST =17:40 FREQ=11527 1.20 SYN= 103.460 FB=0.2500 SB=3
SCAN = 37 GLD554

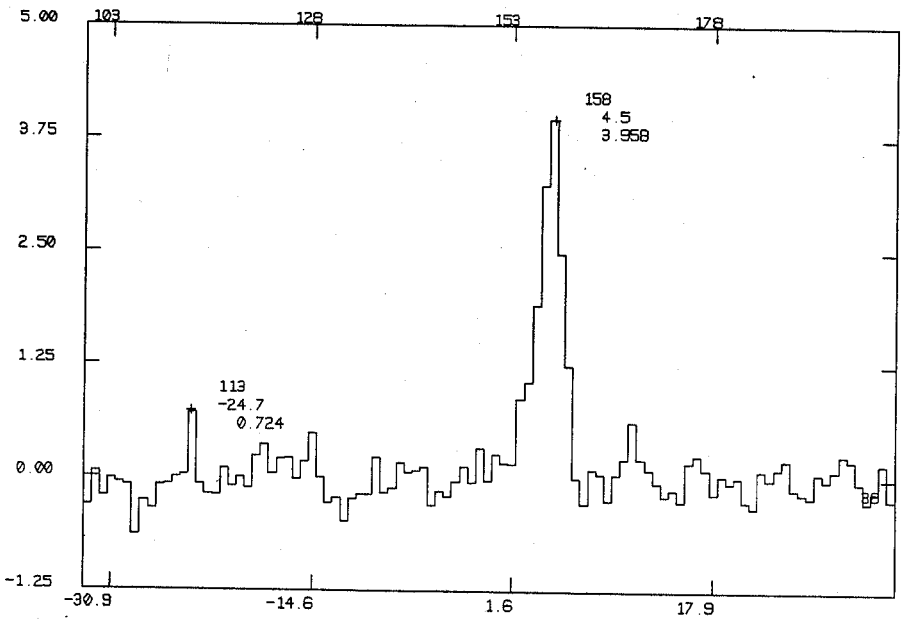
5.00
3.75
2.50
1.25
0.00
-1.25
103
128
153
178
158
4.5
3.958
113
-24.7
0.724
-30.9
-14.6
1.6
17.9
38
DATE 6- 2-92 IST =18: 6 FREQ=11527 1.20 SYN= 103.458 FB=0.2500 SB=3
SCAN = 38 GLD546

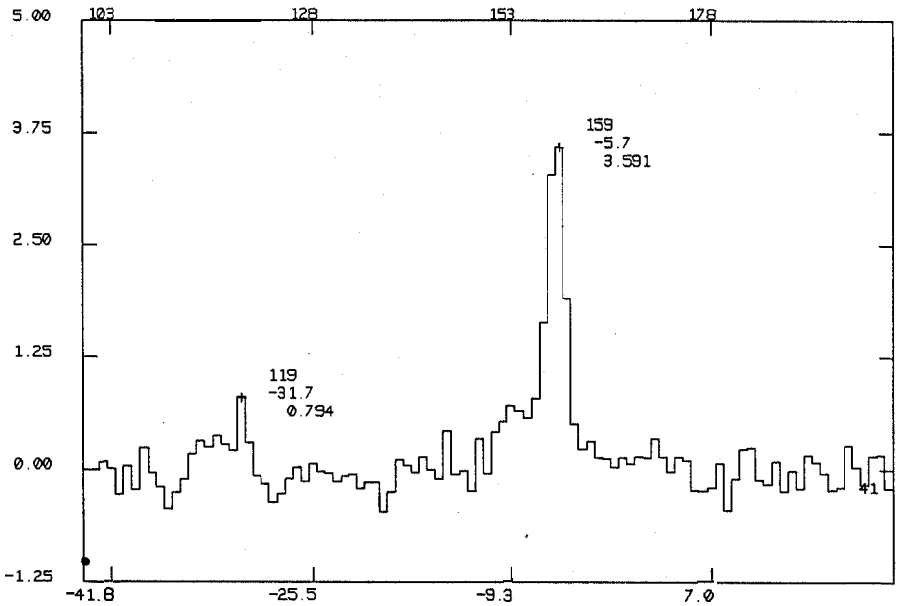

DATE 6- 2-92 IST =18:55 LO=115271.20 SYN= 103.459 FB=0.2500 B=3

SCAN = 41 GLD556

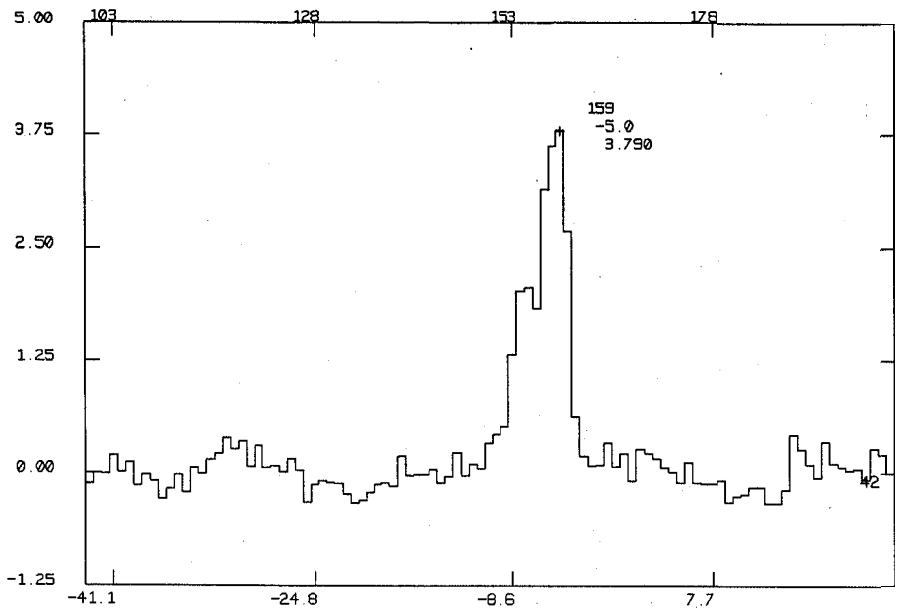

DATE 6- 2-92 IST =19:32 FREQ=115271.20 SYN= 103.459 FB=0.2500 SB=3

SCAN = 42 GLD557

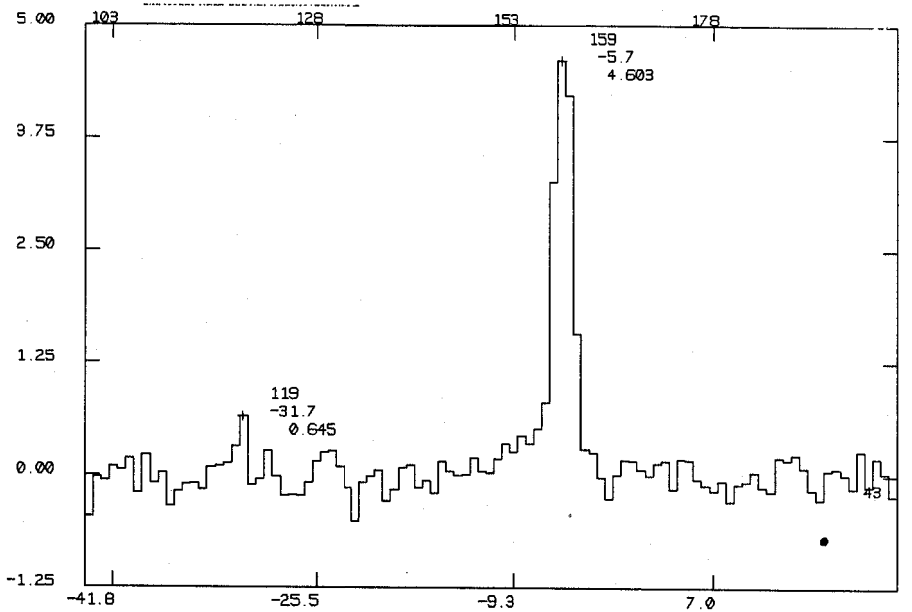

DATE 6- 2-92 IST =19:48 FREQ=115271.20 SYN= 103.459 FB=0.2500 SB=3

SCAN = 43 GLD558

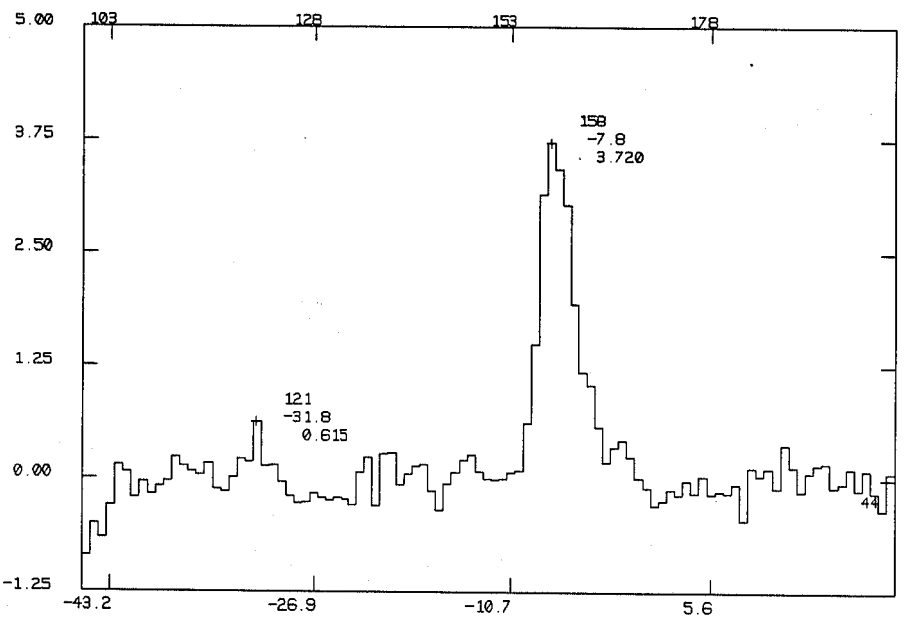

DATE 6- 2-92 IST =20: 5 FREQ=115271.20 SYN= 103.460 FB=0.2500 SB=3

SCAN = 44 GLD559

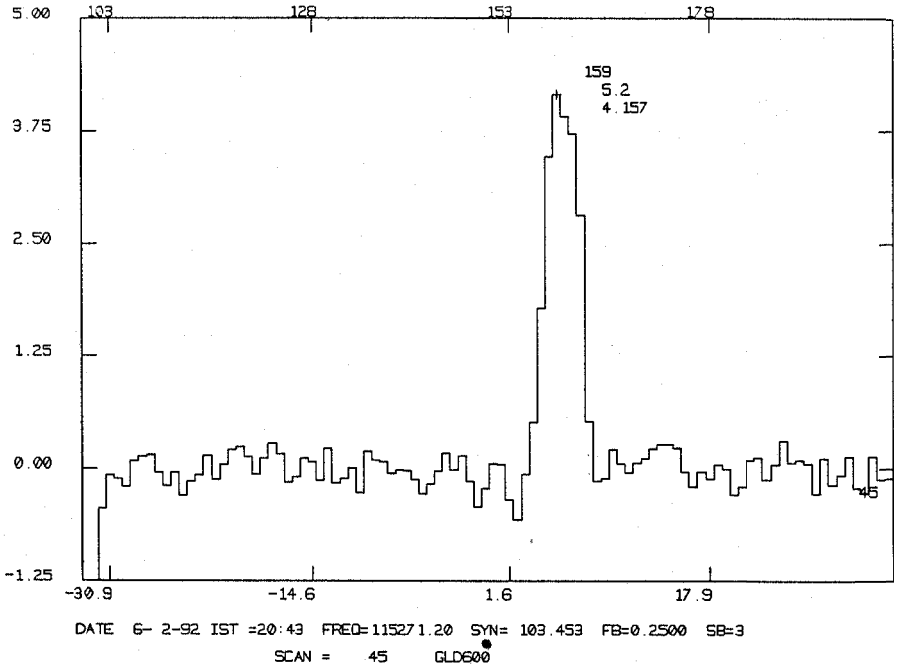
5.00
3.75
2.50
1.25
0.00
-1.25
103
128
153
178
159
5.2
4.157
45
-30.9
-14.6
1.6
17.9
DATE 6- 2-92 IST =20:43 FREQ=115271.20 SYN= 103.453 FB=0.2500 SB=3
SCAN = 45 GLD600

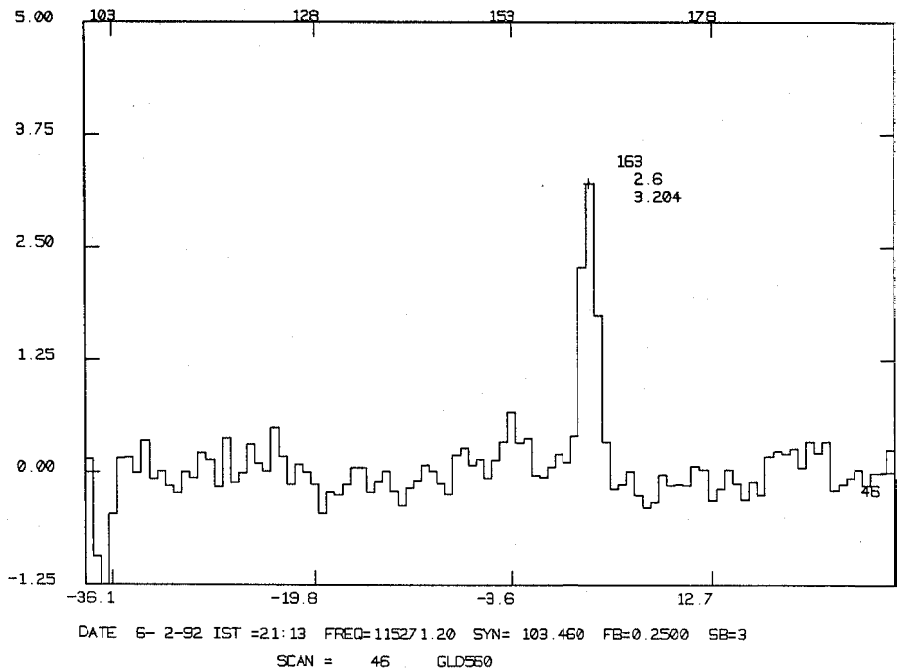
5.00
3.75
2.50
1.25
0.00
-1.25
103
128
153
178
163
2.6
3.204
46
-36.1
-19.8
-3.6
12.7
DATE 6- 2-92 IST =21:13 FREQ=115271.20 SYN= 103.460 FB=0.2500 SB=3
SCAN = 46 GLD560

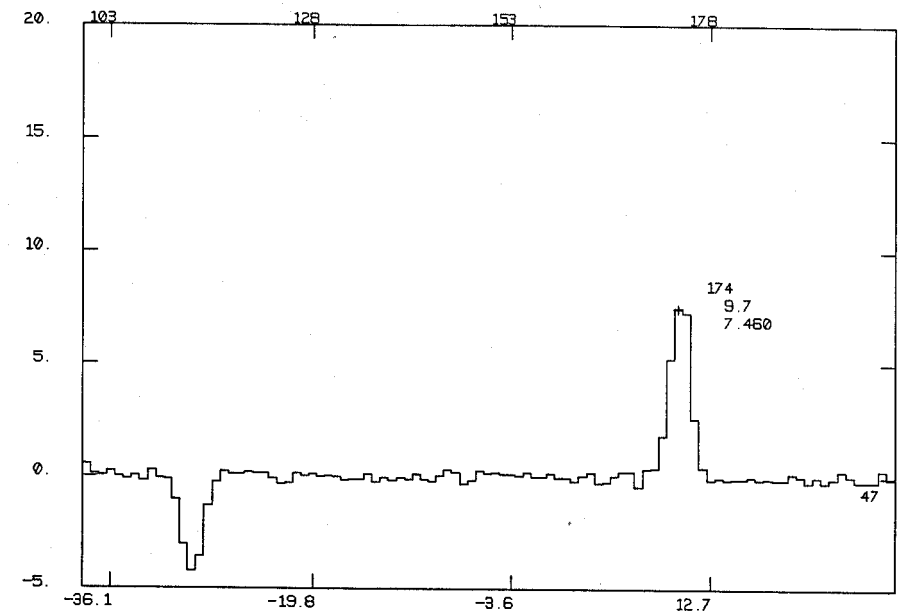

DATE 6- 2-92 IST =21:31 FREQ=11527 1.20 SYN= 103.455 FB=0.2500 SB=3

SCAN = 47 GLD616

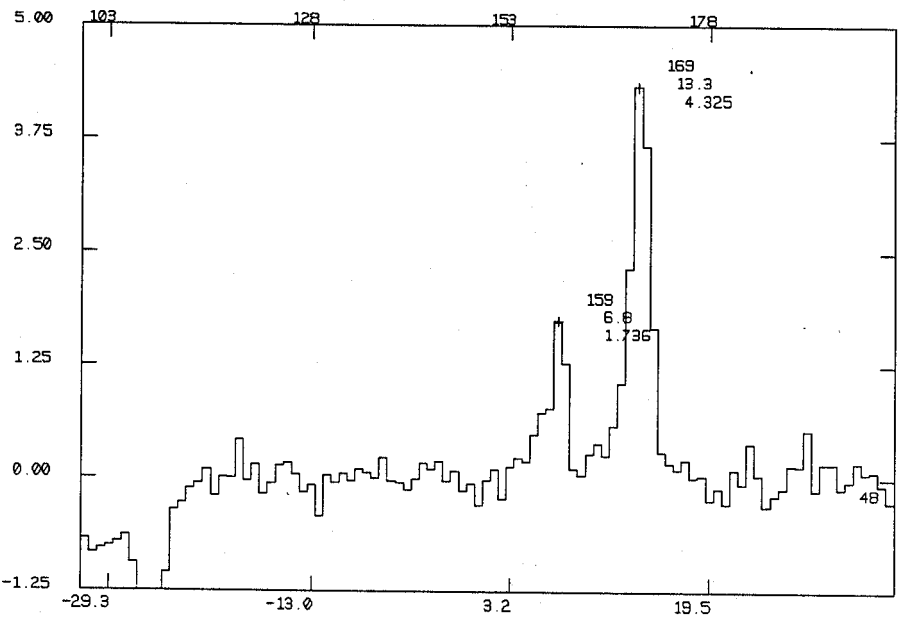

DATE 6- 2-92 IST =21:51 FREQ=11527 1.20 SYN= 103.452 FB=0.2500 SB=3

SCAN = 48 GLD637

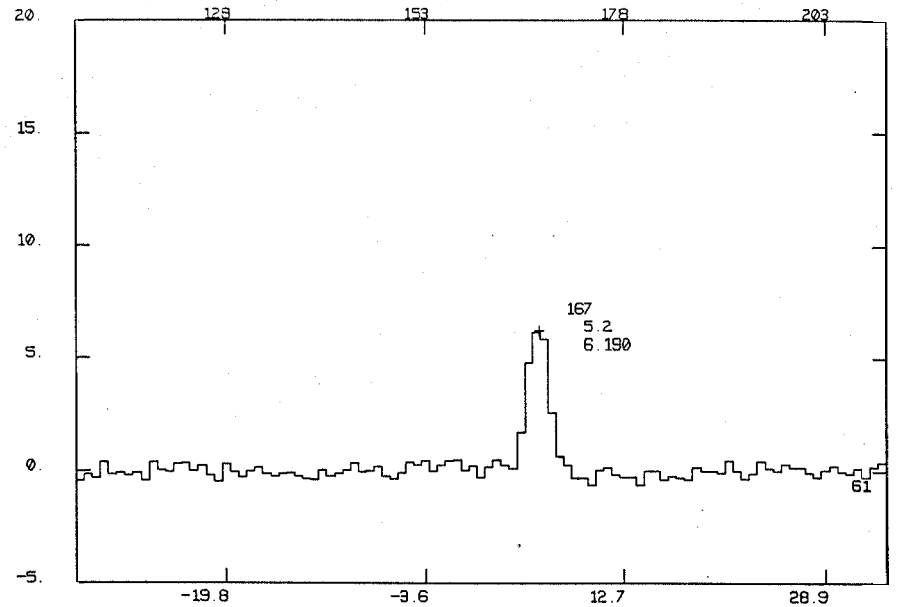
20.
15.
10.
5.
0.
-5.
128
153
178
203
167
5.2
6.190
61
-19.8
-3.6
12.7
28.9
DATE 7- 2-92 IST =11:10 FREQ=115271.20 SYN= 103.476 FB=0.2500 SB=3
SCAN = 61 SDC446

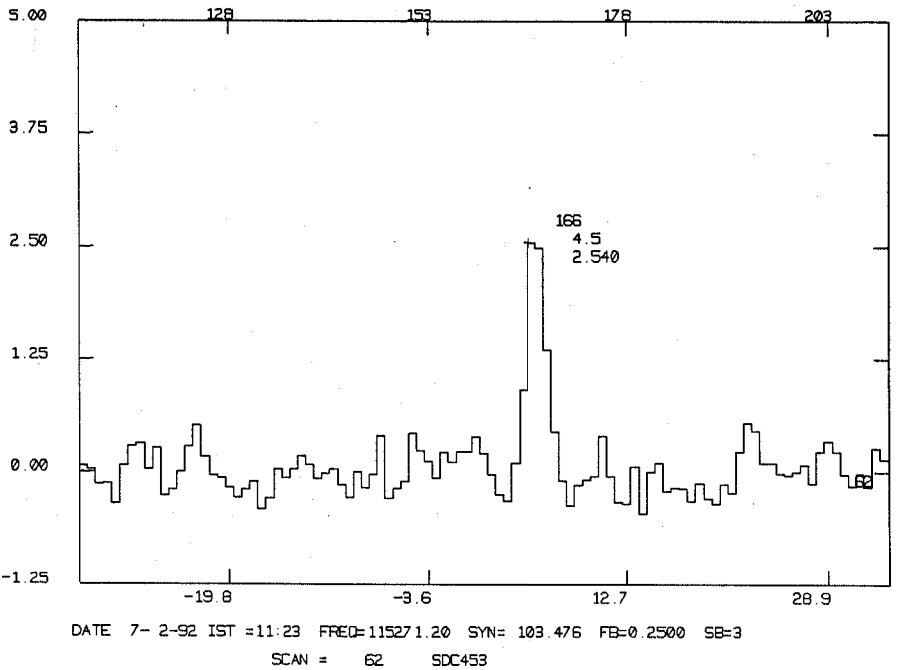
5.00
3.75
2.50
1.25
0.00
-1.25
128
153
178
203
166
4.5
2.540
62
-19.8
-3.6
12.7
28.9
DATE 7- 2-92 IST =11:23 FREQ=115271.20 SYN= 103.476 FB=0.2500 SB=3
SCAN = 62 SDC453

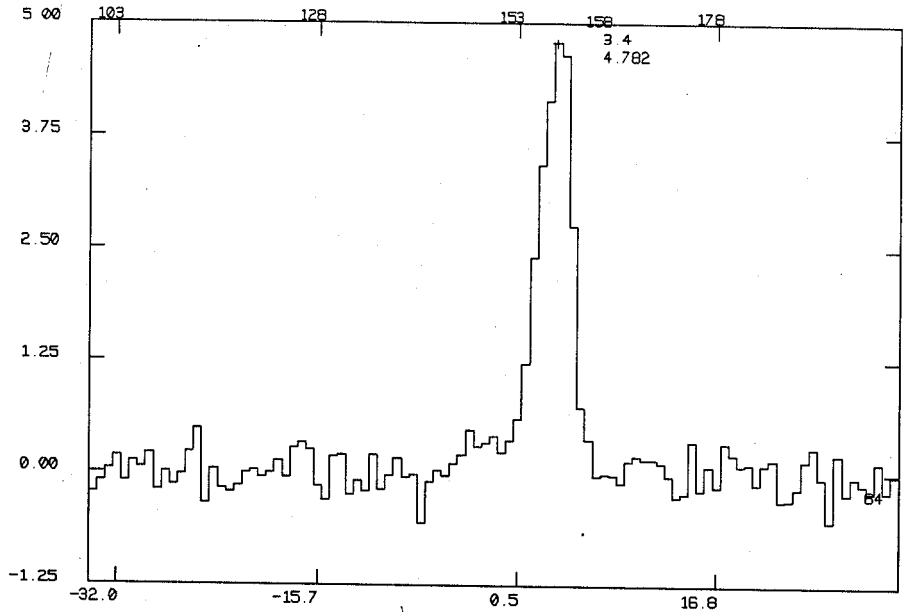
5.00
3.75
2.50
1.25
0.00
-1.25
103
128
153
158
178
3.4
4.782
64
-32.0
-15.7
0.5
16.8
DATE 7- 2-92 IST =13:44 FREQ=115271.20 SYN= 103.468 FB=0.2500 SB=3
SCAN = 64 GLD347

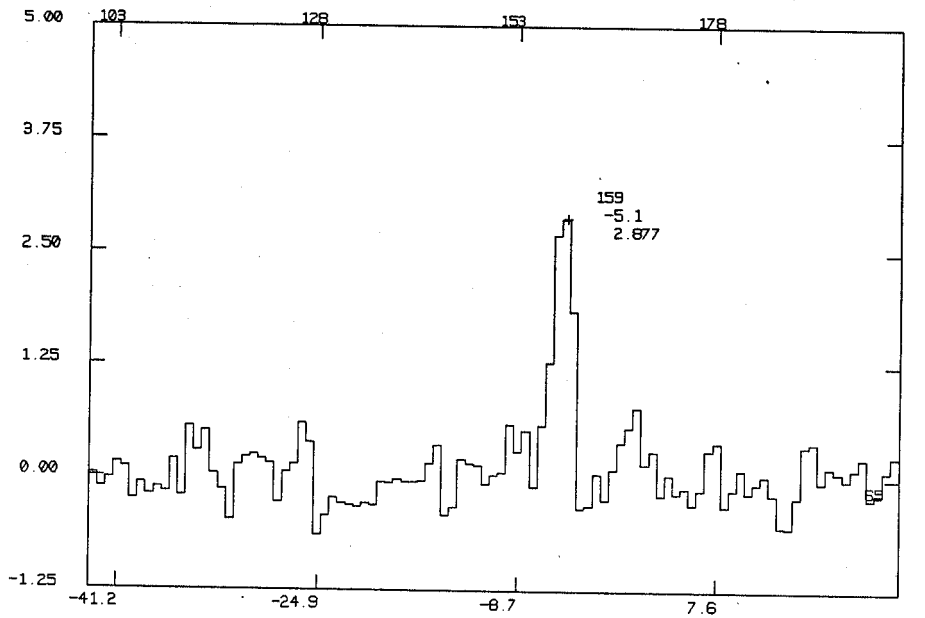
5.00
3.75
2.50
1.25
0.00
-1.25
103
128
153
178
159
-5.1
2.877
65
-41.2
-24.9
-8.7
7.6
DATE 7- 2-92 IST =14: 2 FREQ=115271.20 SYN= 103.470 FB=0.2500 SB=3
SCAN = 65 GLD410

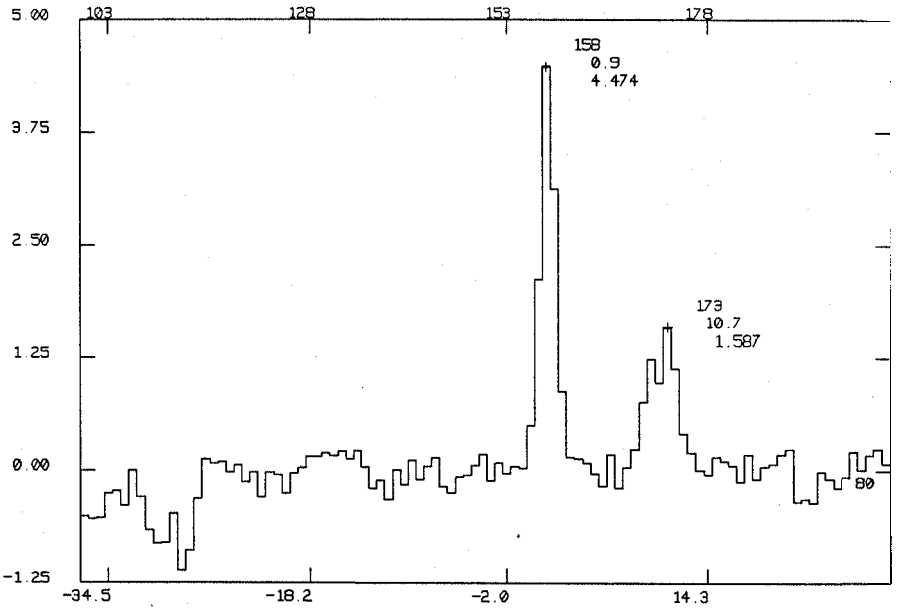
5.00
3.75
2.50
1.25
0.00
-1.25
103
128
153
178
158
0.9
4.474
173
10.7
1.587
80
-34.5
-18.2
-2.0
14.3
DATE 7- 2-92 IST =20:35 FREQ=11527 1.20 SYN= 103.454 FB=0.2500 SB=3
SCAN = 80 GLD627

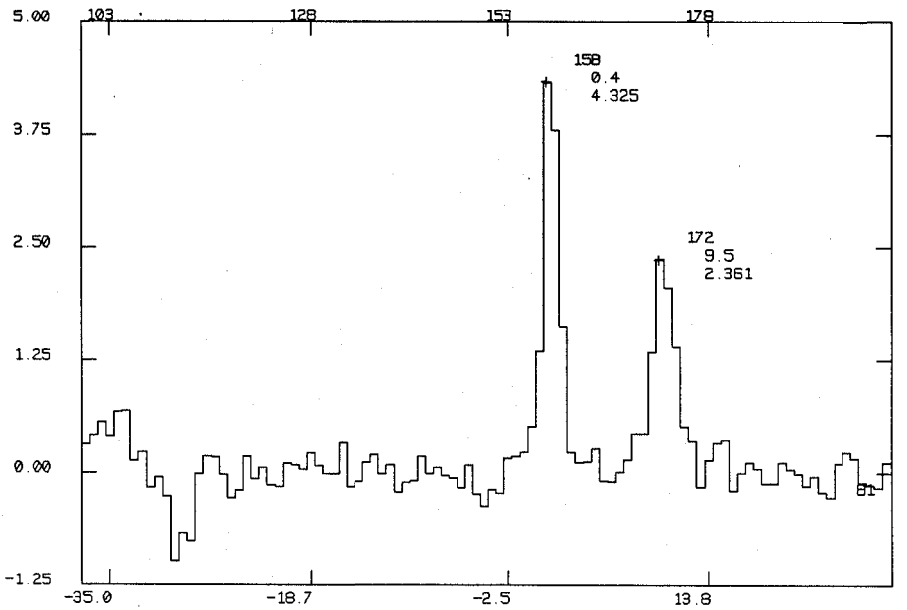
5.00
3.75
2.50
1.25
0.00
-1.25
103
128
153
178
158
0.4
4.325
172
9.5
2.361
81
-35.0
-18.7
-2.5
13.8
DATE 7- 2-92 IST =20:49 FREQ=11527 1.20 SYN= 103.455 FB=0.2500 SB=3
SCAN = 81 GLD624

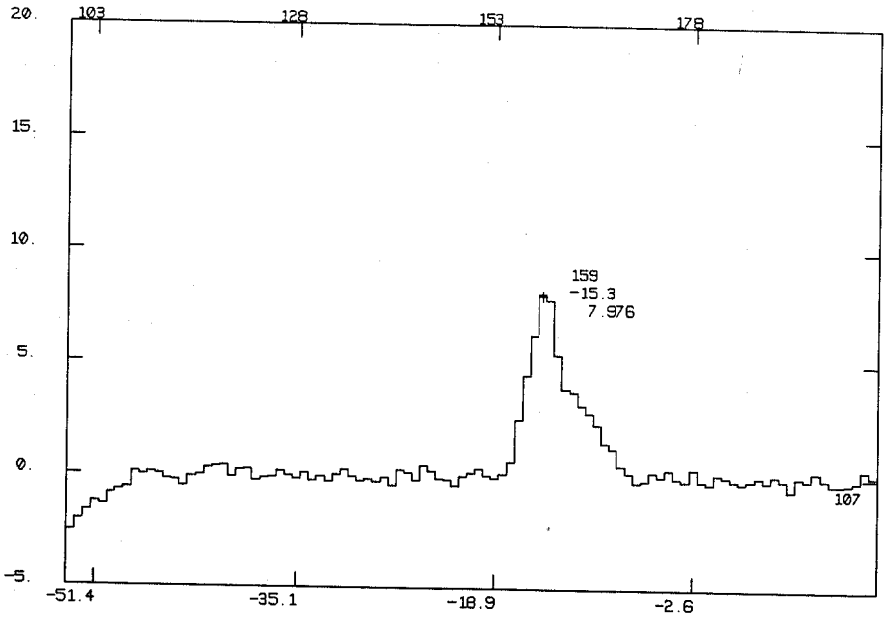

DATE 8- 2-92 IST =16:46 FREQ=115271.20 SYN= 103.469 FB=0.2500 SB=3

SCAN = 107 GLD484

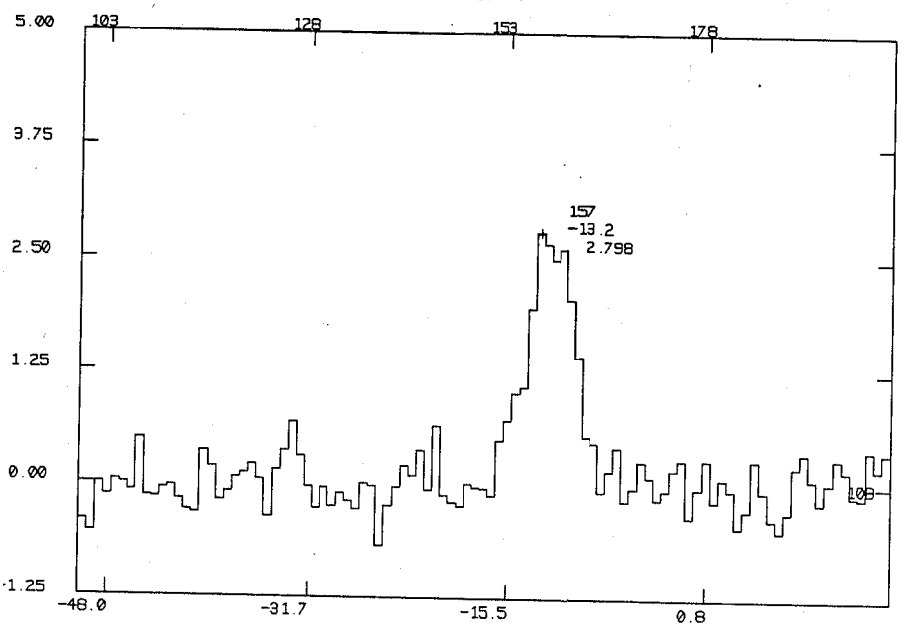

DATE 8- 2-92 IST =17: 1 FREQ=115271.20 SYN= 103.467 FB=0.2500 SB=3

SCAN = 108 GLD485

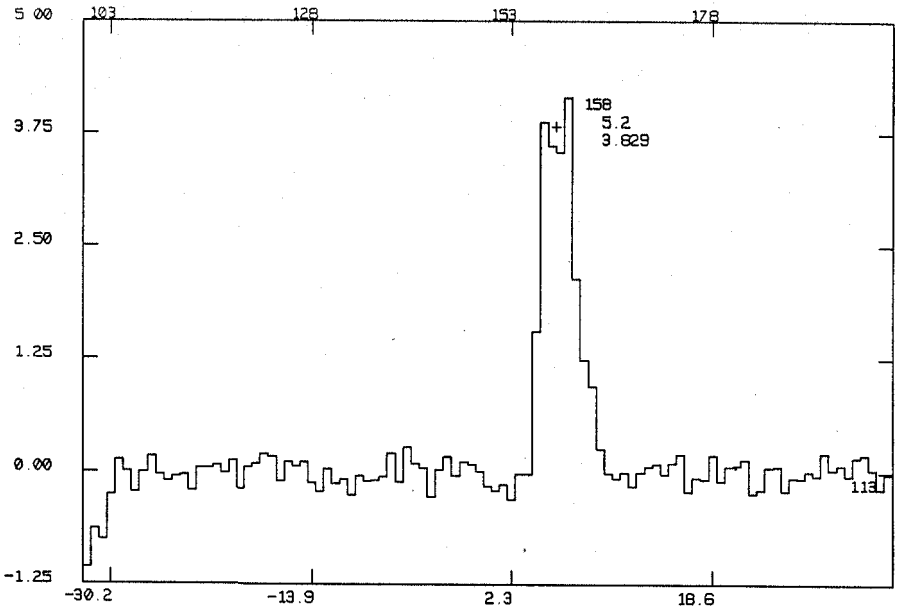
5.00
3.75
2.50
1.25
0.00
-1.25
103
128
153
178
158
5.2
3.829
113
-30.2
-13.9
2.3
18.6
DATE 8- 2-92 IST =19:47 FREQ=11527 1.20 SYN= 103.453 FB=0.2500 SB=3
SCAN = 113 GLD590

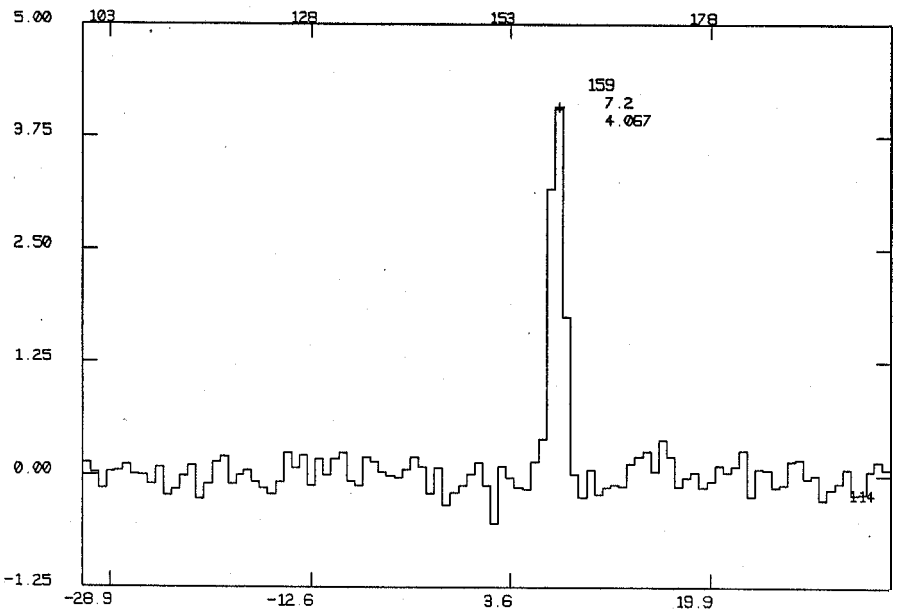
5.00
3.75
2.50
1.25
0.00
-1.25
103
128
153
178
159
7.2
4.067
114
-28.9
-12.6
3.6
19.9
DATE 8- 2-92 IST =20:19 FREQ=11527 1.20 SYN= 103.453 FB=0.2500 SB=3
SCAN = 114 GLD606

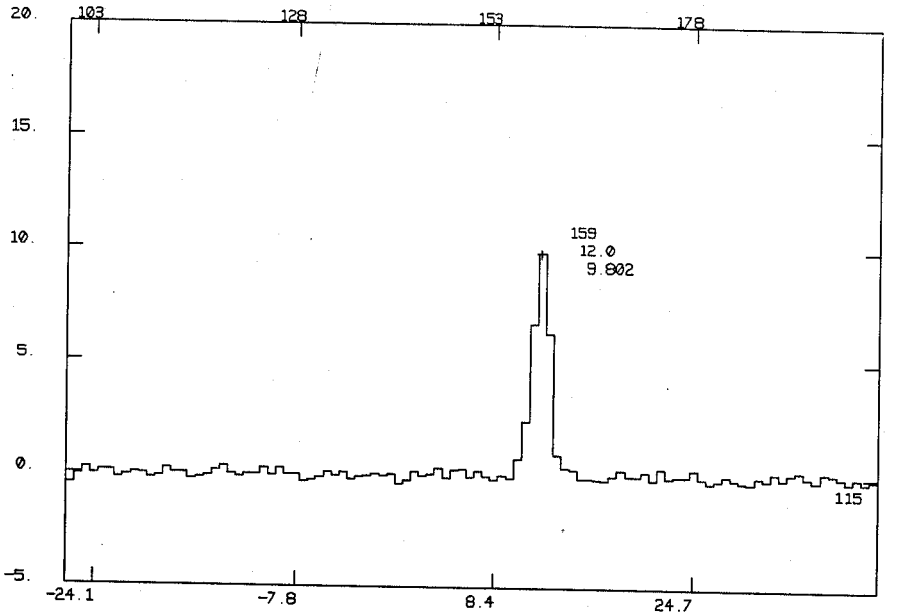
20.
15.
10.
5.
0.
-5.
103
128
153
178
159
12.0
9.802
115
-24.1
-7.8
8.4
24.7
DATE 8- 2-92 IST =21:25 FREQ=115271.20 SYN= 103.450 FB=0.2500 SB=3
SCAN = 115 GLD622

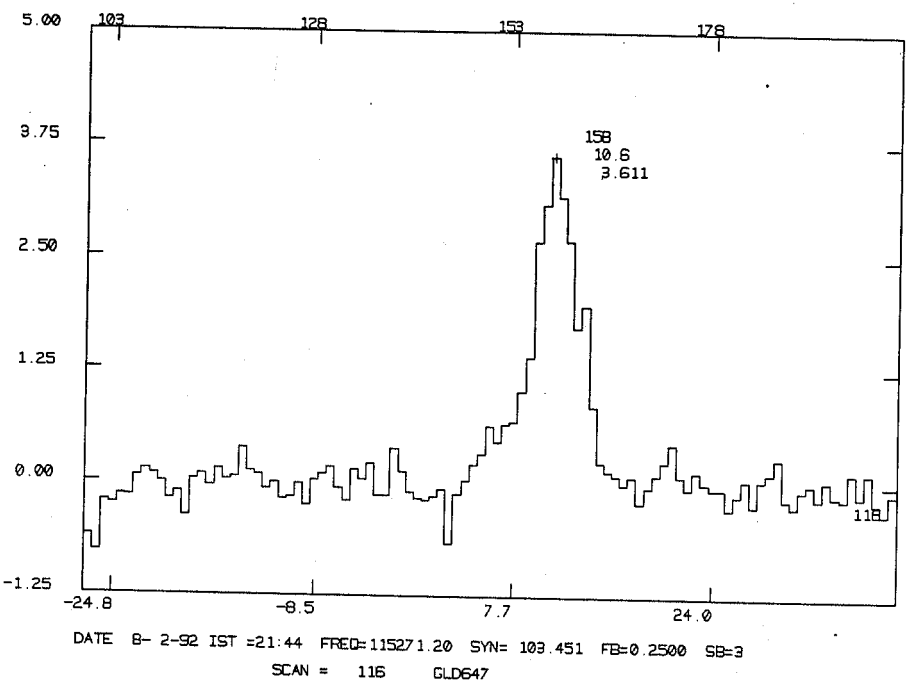
5.00
3.75
2.50
1.25
0.00
-1.25
103
128
153
178
158
10.6
3.611
118
-24.8
-8.5
7.7
24.0
DATE 8- 2-92 IST =21:44 FREQ=115271.20 SYN= 103.451 FB=0.2500 SB=3
SCAN = 116 GLD647

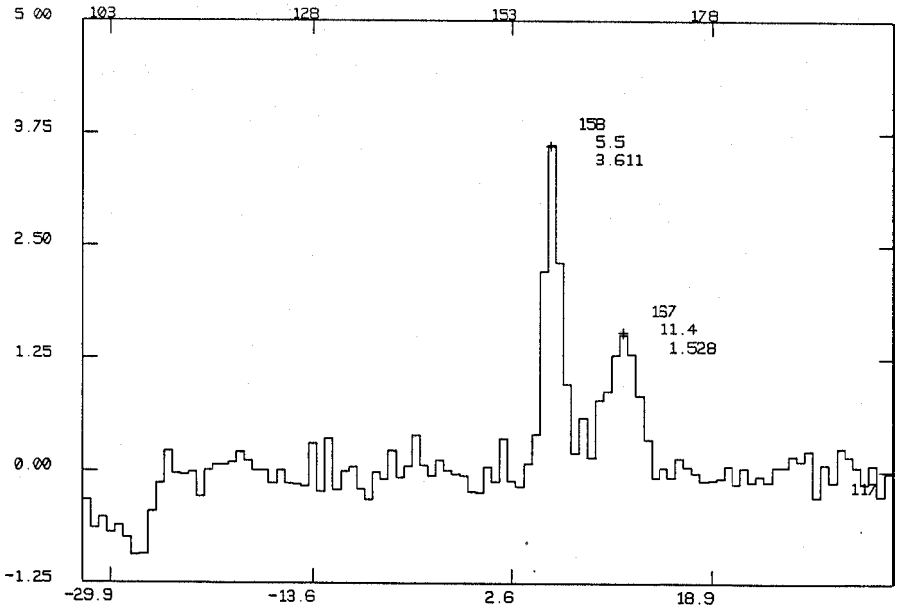

DATE 8- 2-92 IST =21:58 FREQ=115271.20 SYN= 103.453 FB=0.2500 SB=3

SCAN = 117 GLD648

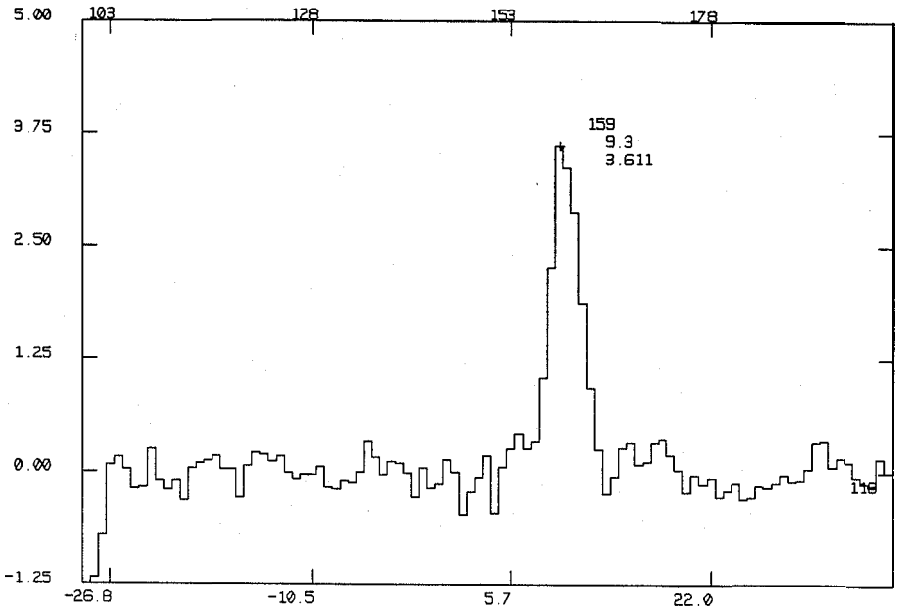

DATE 8- 2-92 IST =22:14 FREQ=115271.20 SYN= 103.454 FB=0.2500 SB=3

SCAN = 118 GLD654

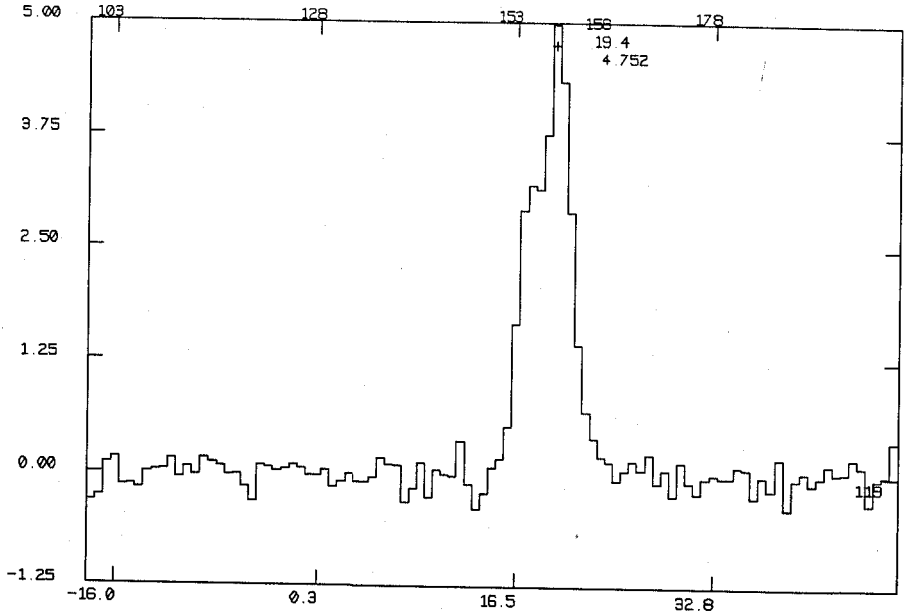

DATE B- 2-92 IST =22:33 FREQ=115271.20 SYN= 103.452 FB=0.2500 SB=3

SCAN = 119 GLD660

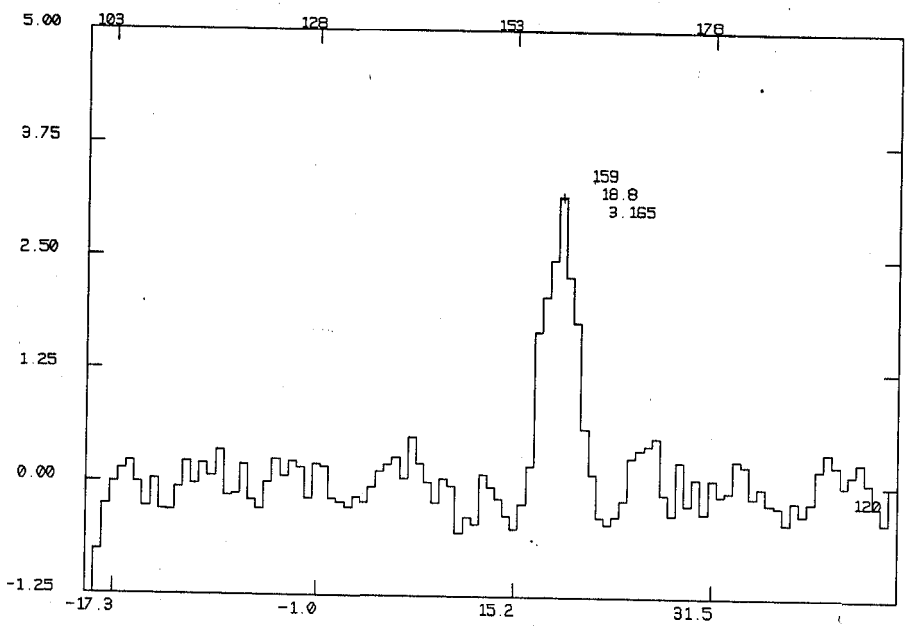

DATE B- 2-92 IST =23: 3 FREQ=115271.20 SYN= 103.453 FB=0.2500 SB=3

SCAN = 120 GLD661

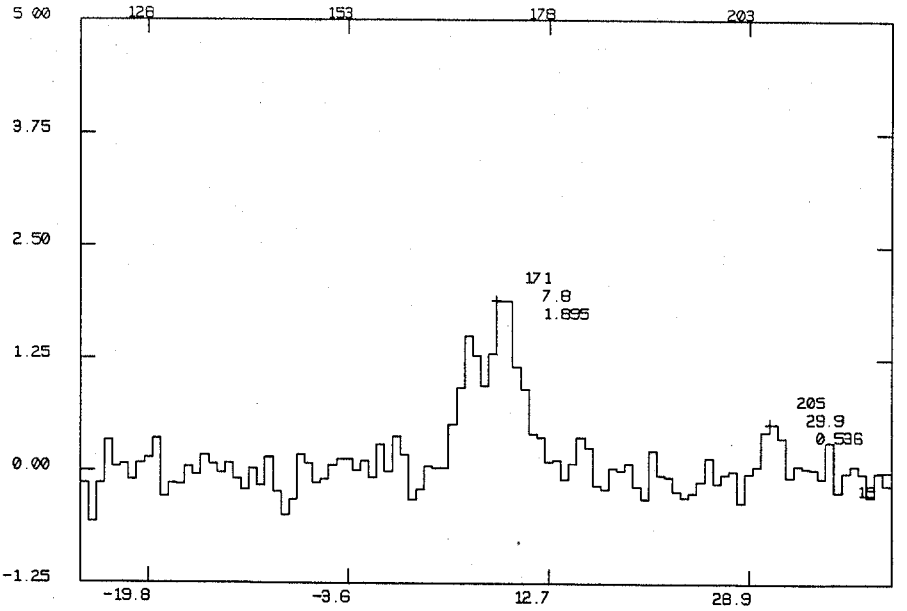
5.00
3.75
2.50
1.25
0.00
-1.25
128
153
178
203
171
7.8
1.895
205
29.9
0.536
-19.8
-3.6
12.7
28.9
DATE 5- 2-92 IST = 9:38 FREQ=11527 1.20 SYN= 103.479 FB=0.2500 SB=3
SCAN = 15 SDC449

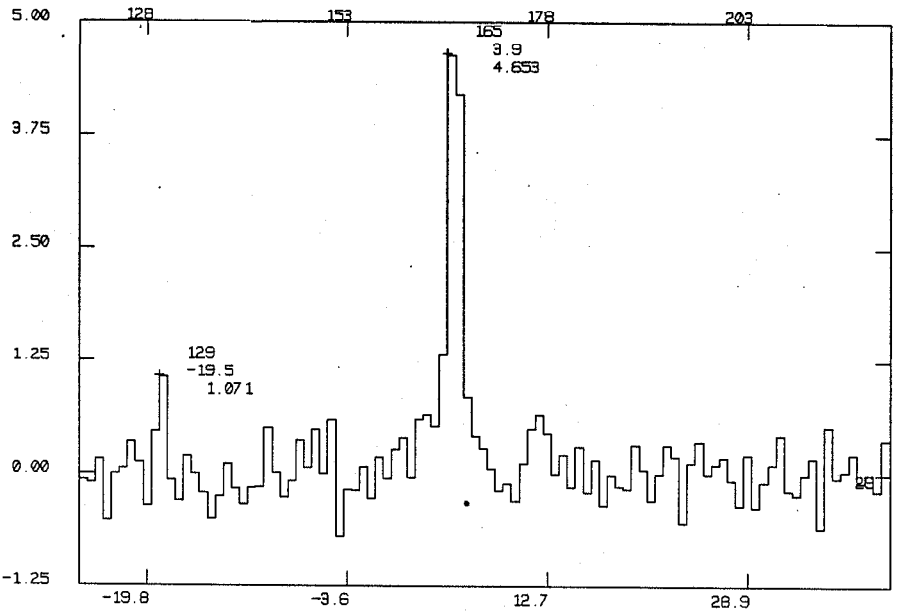
5.00
3.75
2.50
1.25
0.00
-1.25
128
153
178
203
165
3.9
4.653
129
-19.5
1.071
-19.8
-3.6
12.7
28.9
DATE 5- 2-92 IST =23: 7 FREQ=11527 1.20 SYN= 103.462 FB=0.2500 SB=3
SCAN = 29 SDC042

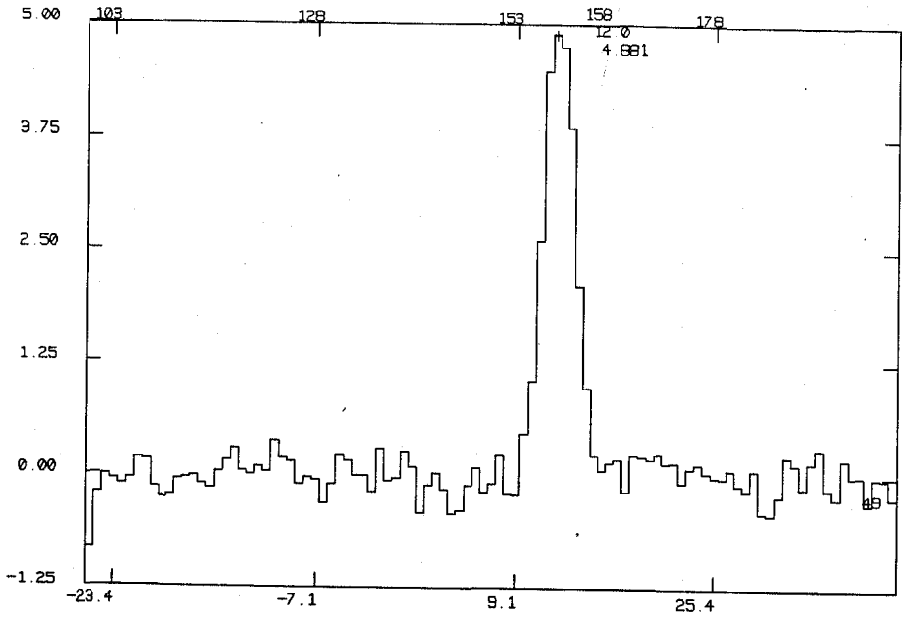
5.00
3.75
2.50
1.25
0.00
-1.25
103
128
153
158
178
12.0
4.881
-23.4
-7.1
9.1
25.4
DATE 6- 2-92 IST =22:20 FREQ=11527 1.20 SYN= 103.451 FB=0.2500 SB=3
SCAN = 49 GLD646

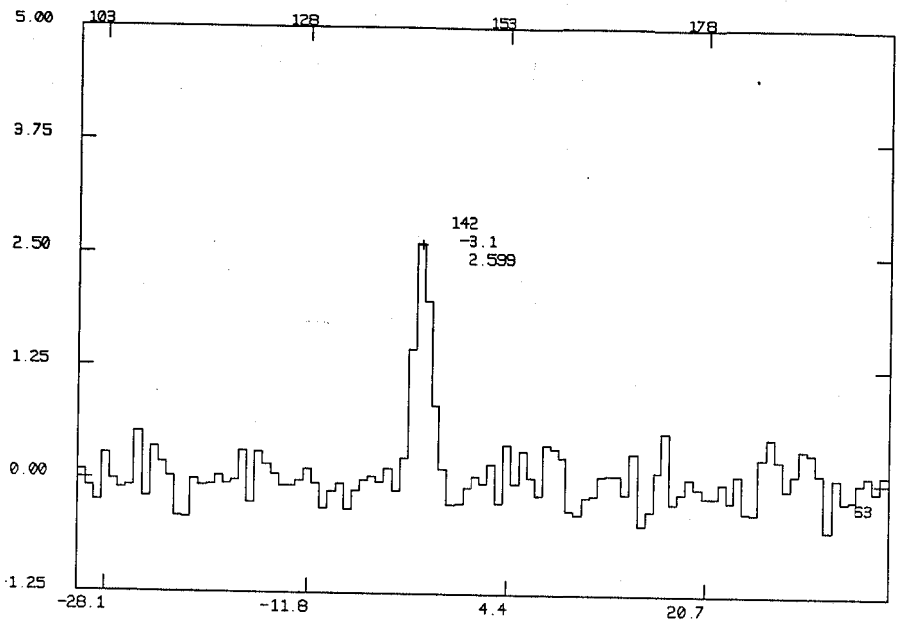
5.00
3.75
2.50
1.25
0.00
-1.25
103
128
153
178
142
-3.1
2.599
-28.1
-11.8
4.4
20.7
DATE 7- 2-92 IST =13:28 FREQ=11527 1.20 SYN= 103.468 FB=0.2500 SB=3
SCAN = 63 GLD362

APPENDIX D : SUMMARYOF THE SIMULATIONS

$15° \leq I \leq 35°$

V_{exp} fixed at 4.5 km s^{-1}

a km s^{-1}	Probability %	R_L (pc)	R_H (pc)
2.5	99	100	400
2.5	99	150	400
2.5	99	250	350
2.5	98	200	400
2.5	92	150	350
2.5	92	150	450
2.5	92	250	400
4.0	64	200	400
7.0	49	100	400

Summary

$V_{exp} = 4.5$ km s^{-1} $\quad \sigma = 2.5$ km s^{-1}

$R_L = 150^{+50}_{-50}$ $\quad R_H = 400^{+50}_{-50}$

$35° \leq I \leq 55°$

V_{exp} fixed at 4.0 km s^{-1}

a km s^{-1}	Probability %	R_L (pc)	R_H (pc)
3.0	100	150	550
3.0	100	300	450
3.0	98	200	500
3.0	98	200	450
3.0	88	250	550
4.5	88	300	450
4.5	88	350	450
1.5	88	150	550

Summary

$V_{exp} = 4.0$ km s^{-1} $\quad \sigma = 3.0$ km s^{-1}

$R_L = 200^{+50}_{-50}$ $\quad R_H = 500^{+50}_{-50}$

$55° \leq l \leq 75°$

γ fixed at 4.0 km s^{-1}

a km s^{-1}	Probability %	R_L (pc)	R_H (pc)
4.0	98	200	300
4.0	98	150	350
4.0	98	200	350
4.0	98	100	400
4.0	98	150	300
4.0	89	100	450
4.0	89	150	400
4.0	89	200	400
6.0	89	150	350
2.0	35	100	350

Summary

$V_{exp} = 4.0$ km s^{-1} a = 4.0 km s^{-1}

$R_L = 100\text{-}150$ $R_H = 400^{+50}_{-50}$

$105° \leq l \leq 125°$

V_{exp} fixed at -3.5 km s^{-1}

a km s^{-1}	Probability %	R_L (pc)	R_H (pc)
6.0	100	100	400
6.0	100	100	450
6.0	100	150	400
6.0	100	200	450
6.0	100	150	450
6.0	88	100	350
6.0	88	100	550
6.0	88	200	500
6.0	88	200	550
6.0	88	150	550

Summary

$V_{exp} = -3.5$ km s^{-1} $\sigma = 6.0$ km s^{-1}

$R_L = 150^{+50}_{-50}$ $R_H = 450^{+50}_{-50}$

SUMMARY OF THE SIMULATIONS

$125° \leq l \leq 145°$

V_{exp} fixed at -4.0 km s^{-1}

σ km s^{-1}	Probability %	R_L (pc)	R_H (pc)
5.5	91	150	550
5.5	91	300	600
5.5	91	250	550
5.5	91	300	500
5.5	91	150	600
5.5	91	300	550
5.5	70	100	550
5.5	70	250	650
5.5	70	200	500
5.5	70	200	650
5.5	70	250	500

Summary

$V_{exp} = -4.0$ km s^{-1} $\quad \sigma = 5.5$ km s^{-1}

$R_L = 250^{+50}_{-50}$ $\quad R_H = 550$-600

$145° \leq l \leq 165°$

V_{exp} fixed at 4.0 km s^{-1}

σ km s^{-1}	Probability %	R_L (pc)	R_H (pc)
5.0	92	200	650
5.0	92	350	550
5.0	92	300	550
5.0	92	350	500
5.0	92	200	600
5.0	77	300	600
5.0	77	400	550
5.0	77	250	600
5.0	77	350	600
7.0	77	350	550

Summary

$V_{exp} = 4.0$ krn s^{-1} $\quad \sigma = 5.0$ km s^{-1}

$R_L = 250^{+50}_{-50}$ $\quad R_H = 600^{+50}_{-50}$

$195° \leq l \leq 215°$

V_{exp} fixed at 2.5 km s^{-1}

a km s^{-1}	Probability %	R_L (pc)	R_H (pc)
4.5	100	250	600
4.5	100	350	550
4.5	100	250	550
4.5	100	350	500
4.5	100	200	550
4.5	92	300	600
4.5	92	400	550
2.5	92	150	600
2.5	92	250	600
6.5	77	300	550

Summary

$V_{exp} = 2.5$ km s^{-1} a = 4.5 km s^{-1}

$R_L = 250^{+50}_{-50}$ R_H = 550-600

$215° \leq l \leq 235°$

V_{exp} fixed at 4.5 km s^{-1}

a km s^{-1}	Probability %	R_L (pc)	R_H (pc)
4.5	100	200	650
4.5	100	300	650
4.5	100	350	700
4.5	100	400	700
6.5	100	300	700
6.5	100	300	750
2.5	100	300	700

Summary

$V_{exp} = 4.5$ km s^{-1} $\sigma = 4.5$ km s^{-1}

$R_L = 300^{+100}_{-100}$ $R_H = 650^{+50}_{-50}$

$235° \leq l \leq 255°$

V_{exp} fixed at 1.0 km s^{-1}

a km s^{-1}	Probability %	R_L (pc)	R_H (pc)
4.5	100	1250	1600
4.5	100	1350	1550
2.5	100	1250	1650
2.5	100	1250	1700
2.5	100	1200	1700
2.5	100	1350	1550
4.0	94	1200	1700
4.0	94	1400	1600

Summary

$V_{exp} = 1.0$ km s^{-1} $\sigma = 4.5$ km s^{-1}

$R_L = 1300^{+100}_{-100}$ $R_H = 1600^{+100}_{-100}$

$285° \leq l \leq 345°$

V_{exp} fixed at 10.0 km s^{-1}

a km s^{-1}	Probability %	R_L (pc)	R_H (pc)
8.0	100	110	360
8.0	91	230	380
8.0	91	260	410
8.0	91	200	500
6.0	91	200	400
6.0	91	260	460
6.0	91	200	350
4.0	70	80	430

Summary

$V_{exp} = 10.0$ km s^{-1} $\sigma = 8.0$ km s^{-1}

$R_L = 150^{+50}_{-50}$ $R_H = 400^{+50}_{-50}$

CONSOLIDATED LIST OF REFERENCES

Allen, C.W. 1976, Astrophysical Quantities, (William Clowes and Sons, London), 209.

Bally, J., Langer, W.D., Wilson, R.W., Stark, A.A., Pound, M.W. 1991, in IAU Symp. No. 147 on Fragmentation of Molecular Clouds and Star Formation, eds. E.Falgarone, F.Boulanger and G.Duvert., Kluwer, Dordrecht, 11.

Bally, J. 1989, in Low Mass Star Formation and pre-main sequence objects in Southern Molecular Clouds, ESO Conference and Workshop Proceedings No. 33, ed.B.Reipurth.

Barnard, E.E. 1927, A Photographic Atlas of Selected Regions of the Milky Way, Carnegie Institution of Washington, D.C..

Bhatt, H.C. 1993, *Mon.Not.R.Astr.Soc.*, 262, 812.

Blaauw, A. 1956, *Astrophys.J.*, 123, 408.

Blaauw,A. 1991, in The physics of star formation and the early stellar evolution, eds. C.J.Lada and N.D.Kylafis, (Kluwer Academic Publ.), p125.

Blanco,V.M. 1956, Astrophys. J., 123,64.

Bonneau, M. 1964, *J.Obs.*, 47, 251.

Cameron, F., Torra, J. 1990, *Astr.Astrophys.*, 241, 57.

Cederblad, S. 1946, Meddelanden fran Lunds Astronomiska Observatorium, Ser.2, 12, No. 119.

Dame, T.M, Ungrechts, H., Cohen, R.S., de Geus, E.J., Grenier, I.A., May, J., Murphy, D.C., Nyman, L.A., Thaddeus, P. 1987, *Astrophys.J.*, 322, 706.

de Vries,C.P., Brand,J., Israel, F.P., de Graauw,Th., Wouterloot, J.G.A., van de Stadt, H., Habing,H.J. 1984, *Astr.Astrophys.Suppl.*, 56, 333.

Dickman, R.L., 1978, *Astrophys.J.Suppl.*, 37, 407.

Dreyer, J.L.E. 1888, New General Catalogue of Nebulae and Clusters of stars, Royal Astronomical Society, London.

Eggen, O.J. 1961, *R.Obs.Bull.* No.41.

Elmegreen,B.G. 1991, in The galactic interstellar medium, eds. W.B. Burton, B.G. Elmegreen, R.Genzel (Saas-Fee advanced course 21), 164.

Elmegreen, B.G. 1987, in Physical Processes in Interstellar Clouds, eds.G.E.Norfill and M.Scholer (NATO ASI C Series Vol.21), 1.

Elmegreen, B.G. 1987, in Physical Processes in Interstellar Clouds, eds.G.E.Norfill and M.Scholer (NATO ASI C Series Vol.21), 105.

Evans II, N.J., Lada, E.A. 1991, in IAU Symposium No.147 on Fragmentation of Molecular Clouds and Star Formation, eds. E.Falgarone, F.Boulanger and G.Duvert, Kluwer, Dordrecht, 293.

Feitzinger, J.V. and Stuwe, J.A. 1984, *Astr.Astrophys.Suppl.*, 58, 365

Feitzinger, J.V. and Stuwe, J.A. 1986, *Astrophys.J.*, 305, 534.

Franco,J., Tenario-Tagle,G., Bodenheimer,P., Rosyczka,M., Mirabel,I.F. 1988, *Astrophys.J.*, 333, 826.

Frogel, J.A., Stothers, R. 1977, *Astron.J.*, 82, 890.

Goldsmith, P.F., Langer, W.D., 1978, Astrophys.J., 222, 881.

Gould, B.A. 1879, *Uranometria* Argentina (P.E.Coni, Buenos Aires) 335.

Hartley, M., Manchester, R.R., Smith, R.M., Trittou, S.B.,Goss, W.M. 1986, Astr. Astrophys. Suppl., 63, 27.

Hartman, J.F. 1904, *Astrophys.J.*, 19, 268.

Hirshfeld, A., Sinnott, R.W. 1985, Sky Catalogue 2000.0, Vol.2, Cambridge Univ. Press, Cambridge.

Indrani, C., Sridharan, T.K. 1994, *J.Astrophys.Astr.*, 14 (in press).

Kerr, F.J., Bowers, P.F., Hendrson, A.P. 1981, *Astr.Astrophys.Suppl.*, 44, 63.

Khavtassi, D.Sh. 1960, Atlas of Galactic Dark Nebulae (Acad.Sci.Georgian SSR, Tiflis).

Kutner,M.L., Machnik,D.E., Tucker,K.D., Dickman,R.L. 1980, *Astrophys.J.*, 237, 734.

Kwan, J. 1979, *Astrophys.J.*, 229, 567.

Lesh, J.R. 1968, *Astrophys.J.Suppl.*, 17, 371.

Lindblad,P.O., Westin,T.N.G. 1985, in Birth and Evolution of massive stars and stellar groups, eds. W.Boland and H.van Woerden, Reidel, Dordrecht, 33.

Lindblad, P.O. 1967, *Bull.Astron.Inst.Neth.*, 19, 34.

Lindblad, P.O., Grape, K., Sandqvist, Aa., Schober, J. 1973, *Astr.Astrophys.*, 24, 309.

Lucke P.B. 1978, *Astr.Astrophys.*, 64, 367.

Lundmark K., Melotte, P.J. 1926, Uppsala *Medd.*No.12.

Lynds, B.T. 1962, *Astrophys.J.Suppl.*, 7, 1.

Margulis, M., Lada, C.J., Young, E.T.1989, *Astrophys.J.*, 345, 906.

May, J., Murphy, D.C., Thaddeus, P. 1988, *Astr.Astrophys.Suppl.*, 73, 51.

Olano, C.A. 1982, *Astr.Astrophys.*, 112, 195.

Oort,J.H., Spitzer,L. 1955, *Astrophys.J.*, 121, 6.

Oort, J.H. 1927, *Bull.Astron.Inst.Neth.*, 3, 275.

Patel,N.A., Xie, T., Goldsmith, P.F. 1993, *Astrophys.J.*, 413, 593.

Patel, N.A. 1990, Ph.D.thesis, Indian Institute of Science, Bangalore.

Petrie,R.M. 1965, Dominion *Astrophys.Obs.Publ.*, 12, 317.

Racine, R. 1968, *Astron.J.*, 73, 223.

Radhakrishnan, V., Murray, J.D., Lockhart, P., Whittle, R.P.J. 1972, Astrophys, J. Suppl., 24, 15.

Radhakrishnan, V., Srinivasan G. 1980, *J.Astrophys.Astr.*, 1, 47.

Sahu, M.S. 1992, Ph.D. thesis, University of Groningen.

Schmidt-Kaler,T. 1965, in Astronomie und Astrophysik, ed. H.H.Voigt, (Springer-Verlag, Berlin), p284.

Scoville, N.Z., Yun, M.S., Clemens, D.P., Sanders, D.B., Waller, W.H. 1987, *Astrophys.J.Suppl.*, 63, 821.

Spitzer, L., Schwarzschild, M. 1951, *Astrophys.J.*, 114, 385.

Spitzer, L. 1978, in Physical processes in the interstellar medium (Wiley, New York), 227.

Sridharan, T.K., 1992, *J.Astrophys.Astr.*, 13, 217.

Stark, A.A. 1984, *Astrophys.J.*, 281, 624.

Stark, A.A., Blitz, L. 1978, *Astrophys.J.(Lett)*, 225, L15.

Stothers, R., Frogel, J.A. 1974, *Astron.J.*, 79, 457.

Taylor, D.K., Dickman, R.L., Scoville, N.Z. 1987, *Astrophys.J.*, 315, 104.

Thomasson, M., Donner, K.J., Elmegreen, B.G. 1991, *Astr.Astrophys.*, 250, 316.

Townes, C.H. 1957, in it IAU Symposium No.4, ed.H.C.van de Hulst, Cambridge, 92.

Trumpler, R.J. 1930, *Publ.Astr.Soc.Pacific*, 42, 214.

van den Bergh, S. 1966, *Astron.J.*, 71, 990.

van den Bergh, S., Herbst, W. 1975, *Astron.J.*, 80, 208.

Westin, T.N.G. 1985, *Astr.Astrophys.Suppl.*, 60, 99.

Wilson, R.W., Jefferts, K.B., Penzias, A.A. 1971, *Astrophys.J.(Letters)*., 161, L43.

Witt, A.N., Schild, R.E. 1986, *Apstrophys.J.Suppl.*, 62, 839.